ENVISAT GOMOS Monthly report: December 2004

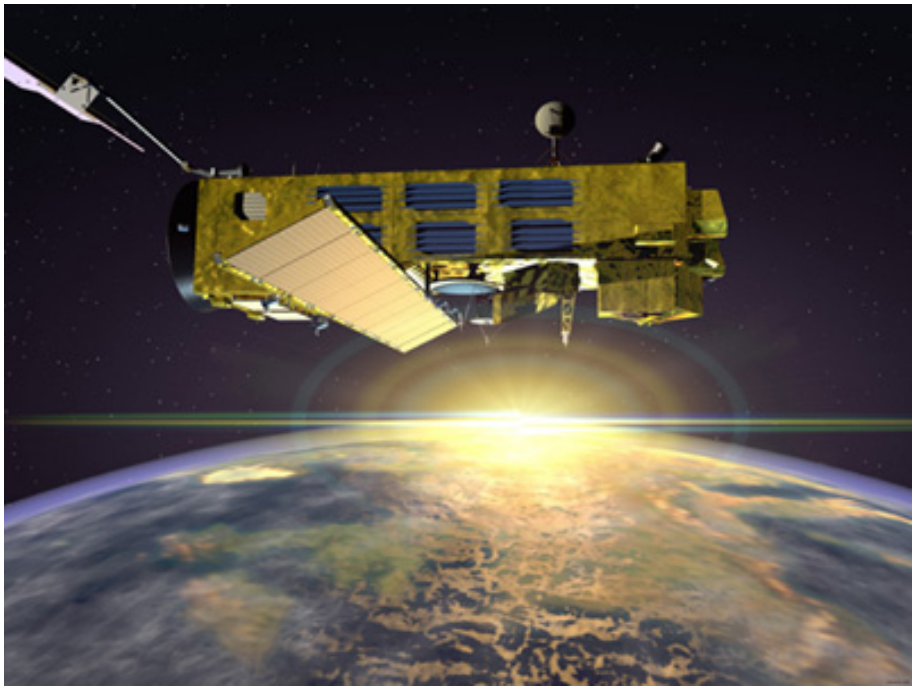

Prepared by:	PCF Team	ESA EOP-GOQ
Inputs from:	GOMOS Quality Working Group, ECMWF	
Issue:	1.0	
Reference:	ENVI-SPPA-EOPG-TN-05-0004	
Date of issue:	24 January 2005	
Status:	Reviewed	
Document type:	Technical Note	
Approved by:	Rob Koopman	

TABLE OF CONTENTS

1 INTRODUCTION

The GOMOS monthly report documents the current status and recent changes to the GOMOS instrument, its data processing chain, and its data products.
The Monthly Report (hereafter MR) is composed of analysis results obtained by the Product Control Facility, combined with inputs received from the different entities working on GOMOS operation, calibration, product validation and data quality. These teams participate in the GOMOS Quality Working Group:

- European Space Agency (ESRIN-PCF, ESOC, ESTEC-PLSO)
- ACRI
- Service d'Aeronomie
- Finnish Meteorological Institute
- IASB-Belgian Institute for Space Aeronomy
- Astrium Space
- ECMWF

In addition, the group interfaces with the Atmospheric Chemistry Validation Team.

1.1 Scope

The main objective of the Monthly Report is to give, on a regular basis, the status of GOMOS instrument performance, data acquisition, results of anomaly investigations, calibration activities and validation campaigns. The following six sections compose the MR:

- Summary
- Unavailability
- Instrument Performance and Configuration
- Level 1 Product Quality Monitoring
- Level 2 Product Quality Monitoring
- Validation Activities and Results

1.2 References

[1] ENVISAT Weekly Mission Operations Report #130, #131, #132, #133 ENVI-ESOC-OPS-RP-1011-TOS-OF
[2] 'Level 1b Detailed Processing Model', PO-RS-ACR-GS-0001, issue 6.1, 28 Nov, 2003
[3] 'Level 2 Detailed Processing Model', PO-RS-ACR-GS-0002, issue 6.0, 6 Feb, 2004
[4] ECMWF GOMOS Monthly Reports

1.3 Acronyms and Abbreviations

ACVT Atmospheric Chemistry Validation Team

ADF	Auxiliary Data File
ADS	Auxiliary Data Server
ANX	Ascending Node Crossing
ARF	Archiving Facility (PDS)
CCU	Central Communication Unit
CFS	CCU Flight Software
CNES	Centre National d'Études Spatiales
CTI	Configuration Table Interface / Configurable Transfer Item
CR	Cyclic Report
DC	Dark Charge
DMOP	Detailed Mission Operation Plan
DPM	Detailed Processing Model
DS	Data Server
DSA	Dark Sky Area
DSD	Data Set Descriptor
ECMWF	European Centre for Medium Weather Forecast
EQSOL	Equipment Switch Off Line
ESA	European Space Agency
ESL	Expert Support Laboratory
ESRIN	European Space Research Institute
ESTEC	European Space Research & Technology Centre
ESOC	European Space Operations Centre
FCM	Fine Control Mode
FMI	Finnish Meteorological Institute
FOCC	Flight Operations Control Centre (ENVISAT)
FP1	Fast Photometer 1
FP2	Fast Photometer 2
GADS	Global Annotations Data Set
GOMOS	Global Ozone Monitoring by Occultation of Stars
GOPR	GOmos PRototype
GS	Ground Segment
HK	Housekeeping
IASB	Institut d'Aeronomie Spatiale de Belgique
IAT	Interactive Analysis Tool
ICU	Instrument Control Unit
IDL	Interactive Data Language
IECF	Instrument Engineering and Calibration Facilities
IMK	Institute of Meteorology Karlsruhe (Meteorologisch Institut Karlsuhe)
INV	Inventory Facilities (PDS)
IPF	Instrument Processing Facilities (PDS)
JPL	Jet Propulsion Laboratory
LAN	Local Area Network
LMA	Levenberg-Marquardt Algorithm
LPCE	Laboratoire de Physique et Chimie de l'Environnement
LUT	Look Up Table
MCMD	Macro Command
MDE	Mechanism Drive Electronics
MIP	Most Illuminated Pixel

MPH	Main Product Header
MPS	Mission Planning System
MR	Monthly Report
OBT	On Board Time
OCM	Orbit Control Manoeuvre
OOP	Out-of-plane
OP	Operational Phase of ENVISAT
PAC	Processing and Archiving Centre (PDS)
PCF	Product Control Facility
PDCC	Payload Data Control Centre (PDS)
PDHS	Payload Data Handling Station (PDS)
PDHS-E	Payload Data Handling Station – ESRIN
PDHS-K	Payload Data Handling Station – Kiruna
PDS	Payload Data Segment
PEB	Payload Equipment Bay
PLSOL	Payload Switch off Line
PMC	Payload Module Computer
PRNU	Pixel Response Non Uniformity
PSO	On-Orbit Position
QC	Quality Control
QUARC	Quality Analysis and Reporting Computer
QWG	Quality Working Group
RIVM	Rijksinstituut voor Volksgezondheid en Milieu
RTS	Random Telegraphic Signal
SA	Service d'Aeronomie
SAA	South Atlantic Anomaly
SATU	Star Acquisition and Tracking Unit
SFA	Steering Front Assembly
SFCM	Stellar Fine Control Mode
SFM	Steering Front Mechanism
SMNA	Servicio Meteorológico Nacional de Argentina
SODAP	Switch On and Data Acquisition Phase
SPA1	Spectrometer A CCD 1
SPA2	Spectrometer A CCD 2
SPB1	Spectrometer B CCD 1
SPB2	Spectrometer B CCD 2
SPH	Specific Product Header
SQADS	Summary Quality Annotation Data Set
SSP	Sun Shade Position
SZA	Solar Zenith Angle

2 SUMMARY

During the reporting period GOMOS instrument had one planned unavailability period on 16th Dec 2004 23:47:00 until 17th Dec 2004 02:35:00 due to a Fine Orbit Control Manoeuvre. For the rest of the period, GOMOS has been operating nominally (section 3.1).

The level 0 availability is high during the reporting period presented a decrease peak on the week 13-19 December. For level 1b data, the availability is less than 80% arriving to 72% during the week 13-19 December (section 3.3).

The detector temperatures during December are around one degree greater than the ones registered during the same period in 2003 (global increase due to the radiator ageing). The expected seasonal variation of the temperatures with amplitude of around one degree can be clearly observed. The peaks that occur mainly in spectrometer B1 and B2 are also to be noted. They happen for some consecutive occultations and every 8-10 days (section 4.3).

A new band setting calibration has been performed during the reporting period with the result that there is no need to change the calibration LUT (section 4.4).

A new spectral calibration exercise has been performed during the reporting period and, as occurred during previous calibrations, the results reach the warning values. The QWG will study the results in depth in order to decide if the auxiliary file should be updated with new values for the wavelength assignment or if these results are coming from the computational method (section 5.3).

On 7th, 13th and 17th December new calibration ADF's were disseminated with updated DC maps of orbits 14480, 14565 and 14622 respectively (section 5.1.2)

3 INSTRUMENT UNAVAILABILITY

3.1 GOMOS Unavailability Periods

In table 3.1-1 there is a list of GOMOS unavailability reports issued during the period 1st December until 31st December 2004. During the reporting period GOMOS was in no-measure mode only due to one planned manoeuvre.

Table 3.1-1: List of unavailability periods issued during the reporting month

Reference of unavailability report	Start time Star orbit	Stop time Stop orbit	Description
EN-UNA-2004/0313	16 Dec 2004 23:47:00.000 Orbit = 14628	17 Dec 2004 02:35:00.000 Orbit = 14629	Planned SFCM

3.2 Stars Lost in Centering

The acquisition of a star initiates with a rallying phase where the telescope mechanism is directed towards the expected position of the star. Subsequently the acquisition procedure enters into detection mode, where the SATU star tracker output signal is pre-processed for spot presence survey and for the location of the most illuminated couple of adjacent pixels for two added lines, over the detection field. The Most Illuminated Pixel (MIP) defines the position of the first SATU centering window. The next step in the acquisition sequence is then initiated and consists of a centering phase where the SATU output signal is pre-processed for spot presence survey over the maximum of 10x10 pixel field. This allows the third phase to begin: the tracking phase.

The centering phase has occasionally resulted in loss of the star from the field of view. The fig. 3.2-1 reports the percentage of the stars lost in centering for the period 03-FEB-2003 to 02-JAN-2005. It can be seen that two stars, mainly weak stars (higher star id means higher magnitude) are lost during centering phase between 5 and 6 % of their planned observations. The star id 115 was lost 40% of the times but it was planned to be occulted five times and was lost twice (in period 26th January – 1st February 2004), so this high percentage of loss is not statistically significant.

As the monitoring shows neither trend nor excessively high percentages of loss, there is no need for the moment to reject any star from the catalogue, and there is no indication of instrument-related problems.

On November 2004 there were reported 10 instances of “target not detected” whereas this month there were two (nominal number of “targets not detected” is one or two per month). This means that the situation came back to the nominal one, being the value of November a temporary phenomenon.

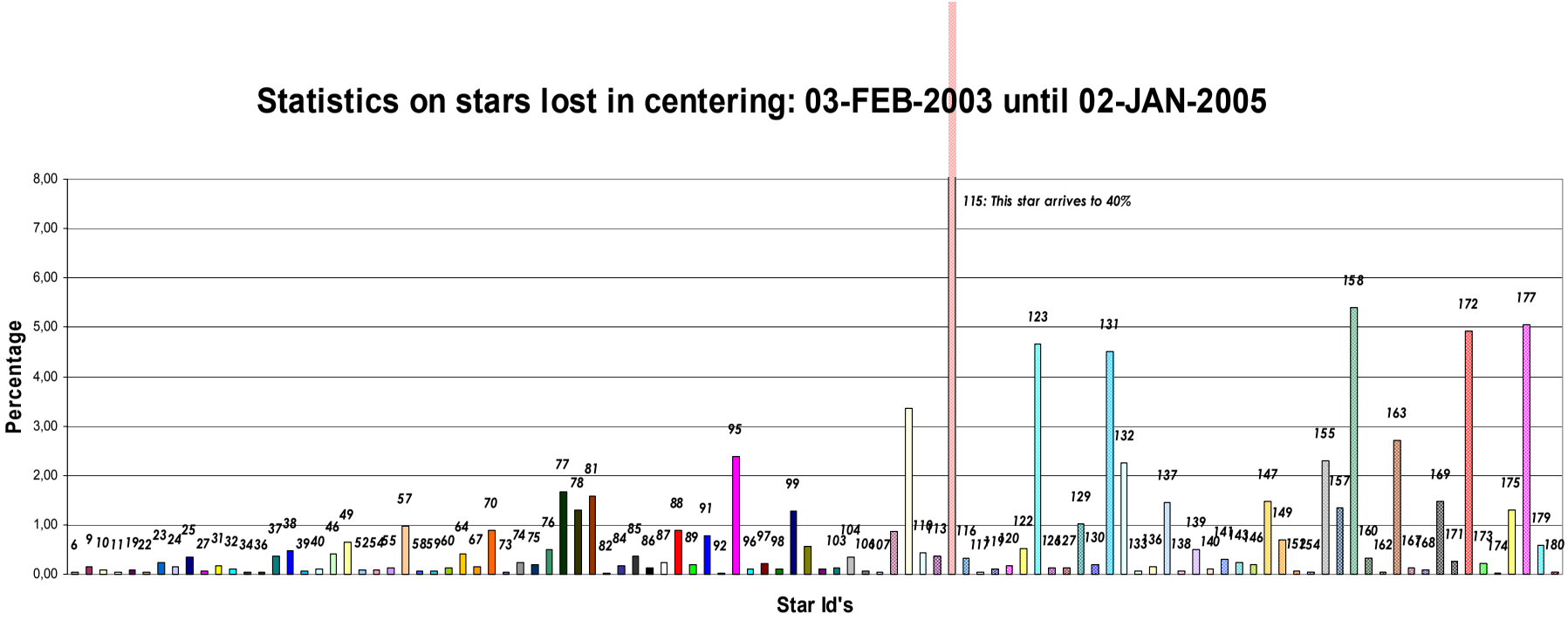

Figure 3.2-1: Statistics on stars that have been lost during the centering phase. The number above the columns correspond to the Star ID

3.3 Data Generation Gaps

The trend in percentage of available data within the archives PDHS-K and PDHS-E is depicted in fig. 3.3-1 (when instrument was in operation). It is a good indicator on how the PDS chain is working in terms of generation and dissemination of data to the archives. The percentage is calculated once per week.

The level 0 availability is high during the reporting period presented a decrease peak on the week 13-19 December. For level 1b data, the availability is less than 80% arriving to 72% during the week 13-19 December.

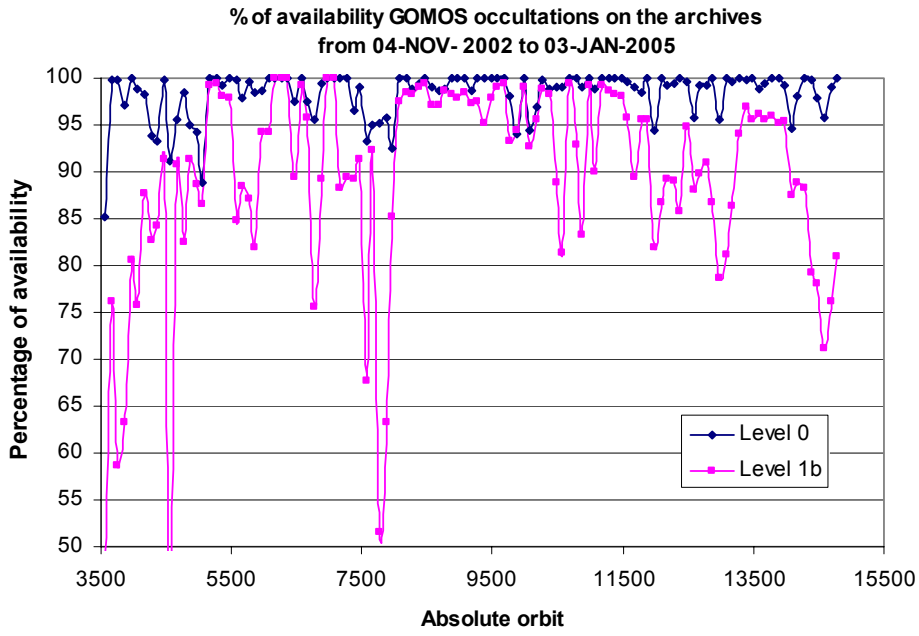

Figure 3.3-1: Percentage of level 0 and level 1b data availability on the archives PDHS-E and PDHS-K

3.3.1 LEVEL 0 PRODUCTS: GOM_NL__0P

Occultations planned to be acquired but for which no GOM_NL__0P data product has become available are presented in fig. 3.3-2 for the reporting period.

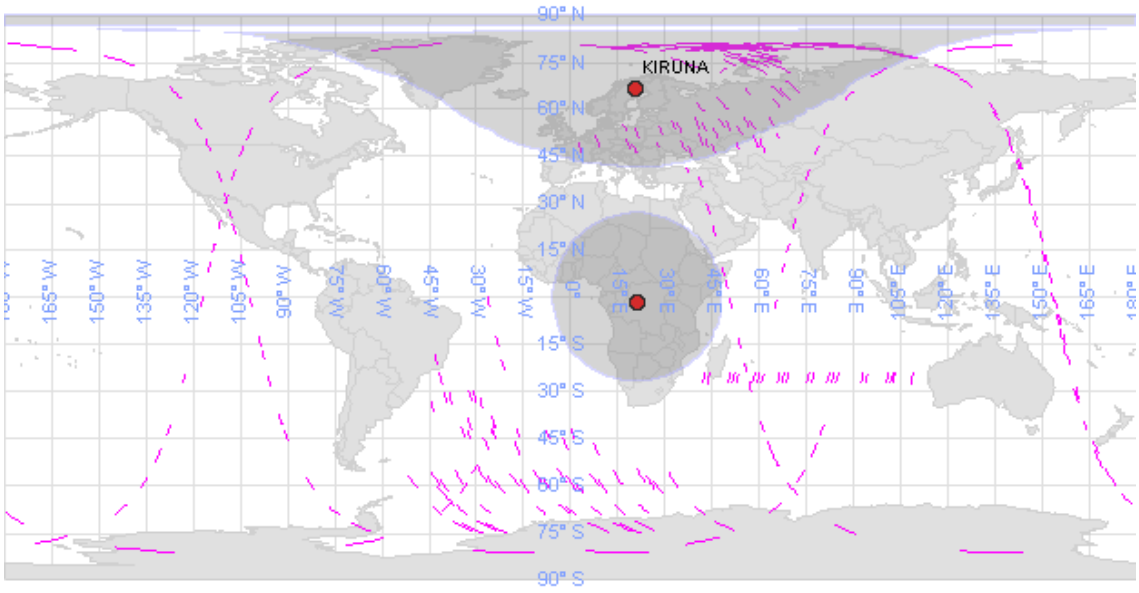

Figure 3.3-2: The pink lines are the orbit segments corresponding to planned data acquisitions for which no GOMOS level 0 product has become available. The grey shadows centered in Kiruna and Svalbard represents the visibility of those acquisition stations

3.3.2 HIGHER LEVEL PRODUCTS

Routine dissemination of higher-level products produced by the PDS to Cal/Val teams and other users is enabled. Currently ESA is also providing products from 2003 that are reprocessed with the prototype processor developed and operated by ACRI.

4 INSTRUMENT CONFIGURATION AND PERFORMANCE

4.1 Instrument Operation and Configuration

During the period end of March 2003 to July 2003 the azimuth range had to be decreased in steps (table 4.1-1) to avoid an instrument problem ("Voice_coil_command_saturation" anomaly) that caused GOMOS to go into STAND BY/REFUSE mode. On July 2003 the driver assembly was switched to the redundant B-side and since that date the full azimuth range (-10.8, +90.8) is again available.

Table 4.1-1: Historical changes in Azimuth configuration

Date	Orbit	Minimum Azimuth	Maximum Azimuth
29-MAR-2003 17:40	5635	0.0	+90.8
31-MAY-2003 06:22	6530	+4.0	+90.8
16-JUN-2003 16:17	6765	+12.0	+90.8
15-JUL-2003 01:39	7200	-10.8	+90.8

The operations of the instrument in other modes than occultation mode are identified in table 4.1-2.

Table 4.1-2: GOMOS operations during the reporting period

UTC time		Start orbit	Stop orbit	Mode (Asynchronous or Synchronous)	Calibration (CAL) or Dark Sky Area (DSA)
03 DEC 2004 23.54.27	49	14442	14449	A	CAL68

There was no new Configurable Table Interface (CTI) uploaded to the instrument. The files used since the beginning of the mission are in table 4.1-3.

Table 4.1-3: Historic CTI Tables

CTI filename	Dissemination to FOCC
CTI_SMP_GMVIEC20030716_123904_00000000_00000004_20030715_000000_20781231_235959.N1	16-JUL-2003
CTI_SMP_GMVIEC20021104_075734_00000000_00000003_20021002_000000_20781231_235959.N1	06-NOV-2003
CTI_SMP_GMVIEC20021002_082339_00000000_00000002_20021002_000000_20781231_235959.N1	07-OCT-2003
CTI_SMP_GMVIEC20020207_154455_00000000_00000000_20020301_032709_20781231_235959.N1	21-FEB-2002

4.2 Limb, Illumination conditions and instrument gain setting

The **limb** and the **illumination condition** are two parameters that can confuse the user community. In table 4.2-1 there are specified the product (level 1b and level 2) parameter where the flag is located, the meaning and the source. The difference between the limb (SPH/bright_limb) and the illumination condition (SUMMARY_QUALITY/limb_flag) is that the first one is coming from the mission scenario and the second is coming from the processing (sun zenith angle computed). The SPH/bright_limb is for some occultations set to "dark" in the mission scenario while they are in fact in bright limb illumination conditions. To select highest quality data for scientific application, data with SUMMARY_QUALITY/limb_flag equal to '0' should be used (see also the disclaimer: http://envisat.esa.int/dataproducts/availability/disclaimers). The instrument gain settings are also specified in table 4.2-1 (they depend on the mission scenario flags) just for information completeness.

Table 4.2-1: Relationship between limb, illumination condition flags and instrument gain settings

Products parameter	Limb: **SPH/bright_limb**	0 = Dark	1 = Bright	Coming from mission scenario
	Illumination Condition: **SUMMARY_QUALITY/limb_flag**	0 = Full Dark 1 = Bright 2 = Twilight	1 = Bright 2 = Twilight	In the geolocation process the sun zenith angle is computed and the occultation then is flagged accordingly
Instrument Gain	SPA Gain	3 (2)	0	Gain setting for spectrometer A. In parenthesis, values valid only for Sirius occultations (starID=1)
	SPB Gain	0	0	Gain setting for spectrometer B

4.3 Thermal Performance

Since the beginning of the mission the hot pixel and RTS phenomena are producing a continuous increase of the dark charge signal within the CCD detectors (see section 4.5.1). In order to minimize this effect, three successive CCD cool down were performed in orbits 800 (25th April 2002), 1050 (13th May 2002) and 2780 (11th September 2002) with a total decrease in temperature of 14 degrees.

Fig. 4.3-1 and 4.3-2 display, respectively, the overall temperature variation and the temperature variation around the Ascending Node Crossing (ANX) time with a resolution of 0.4 degrees (coding accuracy for level 0 data). The CCD temperatures during December are around one degree greater than the ones registered during the same period in 2003 (global increase due to the radiator ageing). The expected seasonal variation of the temperatures with amplitude of around one degree can be clearly observed. The peaks that occur mainly in spectrometer B1 and B2 are also to be noted. They happen for some consecutive occultations and every 8-10 days. Their origin is still not known, as we did not find any correlation between these peaks and other activities carried out by other ENVISAT instruments. The CCD temperature at almost the same latitude location (fig. 4.3-2) is monitored in order to detect any inter-orbital temperature variation.

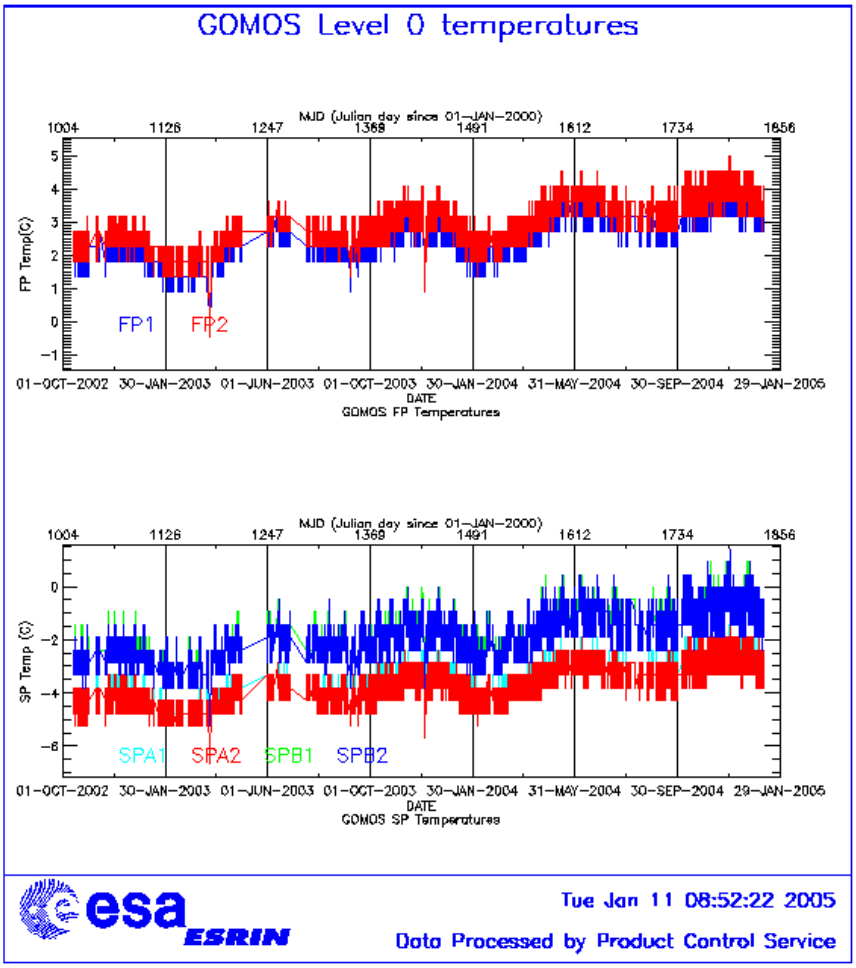

Figure 4.3-1: Level 0 temperature evolution of all GOMOS CCD detectors since October 2002 until the end of the reporting period

The decrease observed on 24th March 2003, twice in September 2003 and at the beginning of December 2003 in all detectors is after GOMOS switch off periods, when the instrument did not have enough time to reach the nominal temperature before starting the measurements.

The orbital temperature variation of the detector SPB2 (fig. 4.3-3 & 4.3-4) is nominal (around 2.5 degrees). The stability of the temperature during the orbit is important because it affects the position of the interference patterns. The phenomenon of the interference is present mainly in SPB and this Pixel Response Non-Uniformity (PRNU) is corrected during the processing.

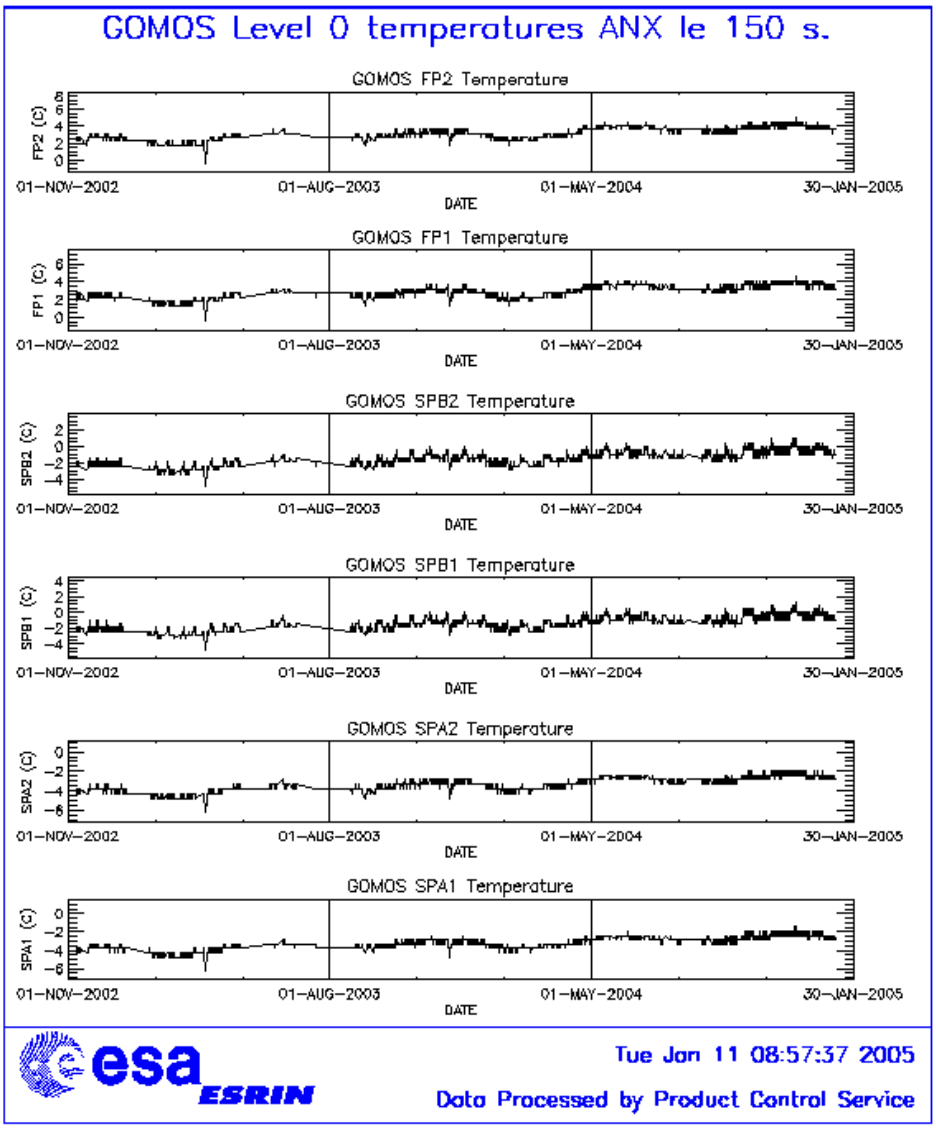

Figure 4.3-2: **Level 0 temperature evolution of all GOMOS CCD detectors around ANX since November 2002 until the end of the reporting period**

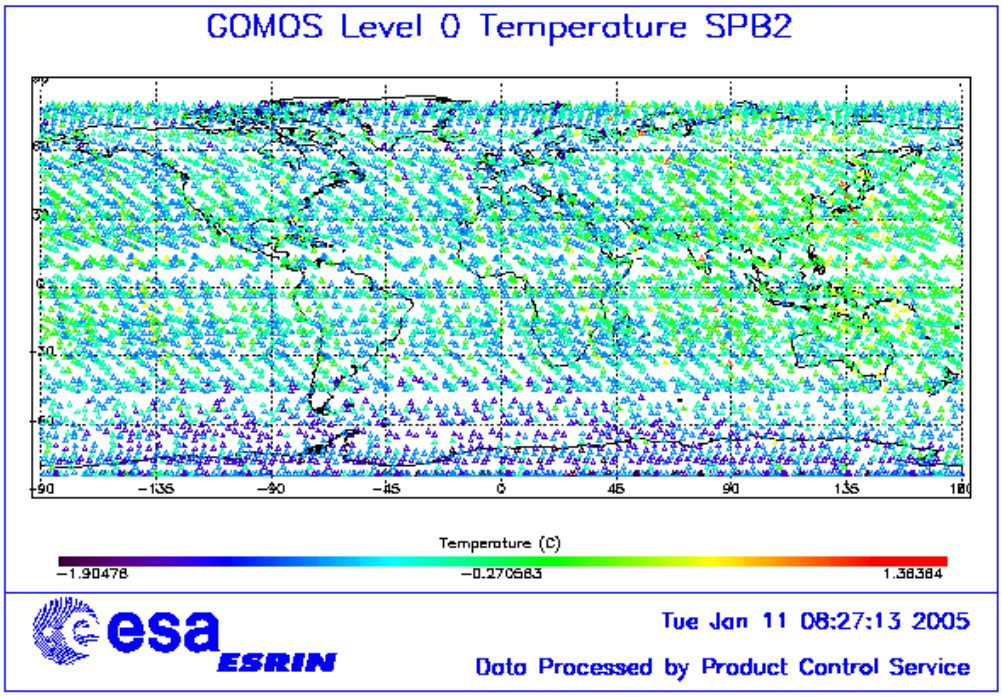

Figure 4.3-3: Ascending orbital variation of SPB2 temperature during reporting period

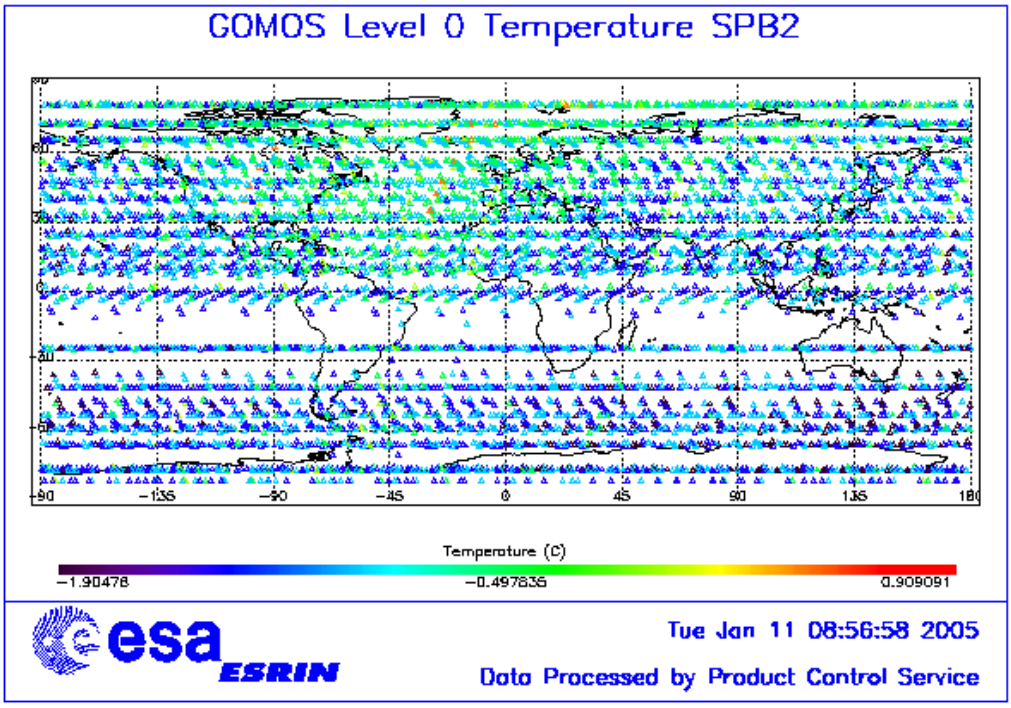

Figure 4.3-4: Descending orbital variation of SPB2 temperature during reporting period

4.4 Optomechanical Performance

A new band setting calibration has been performed during the reporting period with the result that there is no need to change the calibration LUT.

- Version GOMOS/4.00 and previous ones:

In the processors versions of GOMOS GOMOS/4.00 and previous the spectra is expected to be aligned along CCD lines, and therefore use only a single average line index per CCD. In table 4.4-1 the mean values of the location of the star signal for all the calibration analysis done is reported. The 'left' and 'right' values are calculated (the whole interval is not used) because the spectra present a slight slope, more pronounced in the spectrometer B (see fig. 4.4-1). In table 4.4-2, mean values of the location of the star signal are calculated for some specific wavelength intervals. These intervals have been changed between the calibration performed in September 2002 and the ones performed afterwards (until November 2003). Table 4.4-3 reports the average location of the star spot on the photometer 1 and 2 CCD.

- Version GOMOS/4.02:

In the actual processor version (GOMOS/4.02) operational since 23rd March 2004, a Look Up Table (LUT) gives the line index of the spectra location as a function of the wavelength (blue dots in fig. 4.4-1). A new calibration exercise has been performed during December. The position of the stellar spectra of star id 23, 10 and 2 observed in dark-limb spatial spread monitoring mode have been averaged above 120 km altitude and compared to the values of the LUT. The results confirm the LUT values (see table 4.4-4) so for the time being there is no need to update the LUT.

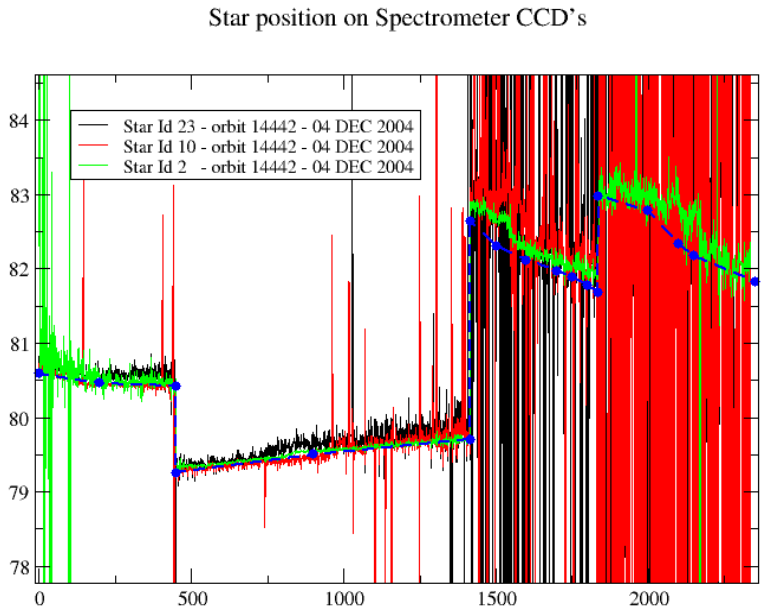

Figure 4.4-1: Average position of star spectra on the CCD

Table 4.4-1: Mean value of the location of the star signal during the occultation at the edges of every band (mean over 50 values, filtering the outliers)

	UV (SPA1) left/right	VIS (SPA2) left/right (Inverted spectra)	IR1 (SPB1) left/right	IR2 (SPB2) left/right
11/09/2002	80.7/80.7	79.8/79.5	82.8/81.9	83.1/82.1
01/01/2003	80.7/80.6	79.8/79.5	82.8/82.0	83.2/82.2
17/07/2003 & 02/08/2003	80.7/80.7	79.8/79.5	82.8/81.9	83.1/82.1
08/11/2003	80.7/80.6	79.8/79.5	82.8/81.9	83.1/82.1

Table 4.4-2: Mean value of the location of the star signal during the occultation (as table 4.4-1) but now within some wavelength intervals

	UV (SPA1)	VIS (SPA2)	IR1 (SPB1)	IR2 (SPB2)
11/09/2002 wl range (nm)	80.8 [300-330]	79.8 [500-530]	82.6 [760-765]	82.9 [937-942]
01/01/2003 wl range (nm)	80.6 [350-360]	78.6 [650-670]	81.6 [760-765]	80.3 [935-945]
02/08/2003	80.6	79.7	82.5	82.8
08/11/2003	80.6	79.9	82.4	82.8

Table 4.4-3: Average column and row pixel location of the star spot on the photometer CCD during the occultation

	FP1 (column/row)	FP2 (column/row)
11/09/2002	11/4	5/5
01/01/2003	10/4	6/4.9
02/08/2003	10/4	6/5
08/11/2003	10/4	6/5
04/12/2004	10/4	6/5

Table 4.4-4: Location of the star signal on the CCD's (corresponding to fig. 4.4-1)

Pixel Column	LUT (Pixel line)	Calibration on 10-APR-2004	Calibration on 04-DEC-2004
0	**80.59**	80.80	80.67
20	**80.46**	80.60	80.44
449	**80.42**	80.50	80.42
450	**79.25**	79.39	79.30
900	**79.50**	79.63	79.57
1415	**79.70**	79.76	79.76
1416	**82.64**	82.80	82.88
1500	**82.31**	82.60	82.66
1600	**82.12**	82.22	82.30
1700	**81.97**	82.04	82.08
1750	**81.89**	81.98	82.03
1800	**81.78**	81.91	81.96
1835	**81.68**	81.88	81.94
1836	**82.98**	83.10	83.10
2000	**82.78**	82.90	82.94
2100	**82.33**	82.70	82.73
2150	**82.17**	82.40	82.54
2350	**81.83**	82.00	82.00

4.5 Electronic Performance

4.5.1 DARK CHARGE EVOLUTION AND TREND

The trend of Dark Charge (DC) is of crucial importance for the final quality of the products, and is therefore subject to intense monitoring. As part of the DC there is:

- "Hot pixels", a pixel is "hot" when its dark charge exceeds its value measured on ground, at the same temperature, by a significant amount.
- RTS phenomenon (Random Telegraphic Signal), it is an abrupt change (positive or negative) of the CCD pixel signal, random in time, affecting only the DC part of the signal and not the photon generated signal.

The temperature dependence of the DC would make this parameter a good indicator of the DC behaviour, but the hot pixels and the RTS are producing a continuous increase of the DC (see trend in fig. 4.5-1 and 4.5-2). To take into account these phenomena, since version GOMOS/4.00 (actual one is GOMOS/4.02) a DC map per orbit is extracted from a Dark Sky Area (DSA) observation performed around ANX (full dark conditions). For every level 1b product (occultation), the actual thermistor temperature of the CCD is used to convert the DC map measured around ANX into an estimate of the DC at the time (and different temperature) of the actual occultation. When the DSA observation is not available, the DC map inside the calibration product that was measured at a given thermistor reference temperature is used; again, the actual thermistor temperature of the CCD is used to compute the actual map. Table 4.5-1 reports the list of products that used the DC maps inside the calibration file due to the non-availability of DSA observation. A "CAL DC map with no T dep." means that, as the temperature information was not available for that occultation, the DC map used is exactly the one inside the Calibration product.

Table 4.5-1: Table of level 1b products that used the Calibration DC maps instead of the DSA observation

Product name	DC information
GOM_TRA_1PNPDE20041207_202149_000000572032_00415_14497_0000.N1	DC map with no T dep.
GOM_TRA_1PNPDE20041207_202409_000000602032_00415_14497_0001.N1	DC map used
GOM_TRA_1PNPDE20041207_202741_000000642032_00415_14497_0002.N1	DC map used
GOM_TRA_1PNPDE20041207_202940_000000652032_00415_14497_0003.N1	DC map used
GOM_TRA_1PNPDE20041207_203312_000000882032_00415_14497_0004.N1	DC map used
GOM_TRA_1PNPDE20041207_203640_000000612032_00415_14497_0005.N1	DC map used
GOM_TRA_1PNPDE20041207_203915_000000582032_00415_14497_0006.N1	DC map used
GOM_TRA_1PNPDE20041207_204145_000000562032_00415_14497_0007.N1	DC map used
GOM_TRA_1PNPDE20041207_204417_000000582032_00415_14497_0008.N1	DC map used
GOM_TRA_1PNPDE20041207_204611_000000382032_00415_14497_0009.N1	DC map used
GOM_TRA_1PNPDE20041207_204826_000000392032_00415_14497_0010.N1	DC map used
GOM_TRA_1PNPDE20041207_204958_000000372032_00415_14497_0011.N1	DC map used
GOM_TRA_1PNPDE20041207_205200_000000382032_00415_14497_0012.N1	DC map used
GOM_TRA_1PNPDE20041207_205327_000000382032_00415_14497_0013.N1	DC map used
GOM_TRA_1PNPDE20041207_205522_000000512032_00415_14497_0014.N1	DC map used
GOM_TRA_1PNPDE20041207_205714_000000382032_00415_14497_0015.N1	DC map used

GOM_TRA_1PNPDE20041207_210434_000000382032_00415_14497_0016.N1	DC map used
GOM_TRA_1PNPDE20041207_210917_000000352032_00415_14497_0017.N1	DC map used
GOM_TRA_1PNPDE20041207_211213_000000352032_00415_14497_0018.N1	DC map used
GOM_TRA_1PNPDE20041207_211414_000000442032_00415_14497_0019.N1	DC map used
GOM_TRA_1PNPDE20041207_211633_000000412032_00415_14497_0020.N1	DC map used
GOM_TRA_1PNPDE20041208_195242_000000592032_00429_14511_0000.N1	DC map used
GOM_TRA_1PNPDE20041208_195612_000000652032_00429_14511_0001.N1	DC map used
GOM_TRA_1PNPDE20041208_195807_000000682032_00429_14511_0002.N1	DC map used
GOM_TRA_1PNPDE20041208_200138_000000862032_00429_14511_0003.N1	DC map used
GOM_TRA_1PNPDE20041208_200500_000000592032_00429_14511_0004.N1	DC map used
GOM_TRA_1PNPDE20041208_200734_000000572032_00429_14511_0005.N1	DC map used
GOM_TRA_1PNPDE20041208_201002_000000572032_00429_14511_0006.N1	DC map used
GOM_TRA_1PNPDE20041208_201236_000000572032_00429_14511_0007.N1	DC map used
GOM_TRA_1PNPDE20041208_201430_000000412032_00429_14511_0008.N1	DC map used
GOM_TRA_1PNPDE20041208_201647_000000392032_00429_14511_0009.N1	DC map used
GOM_TRA_1PNPDE20041208_201824_000000372032_00429_14511_0010.N1	DC map used
GOM_TRA_1PNPDE20041208_202027_000000382032_00429_14511_0011.N1	DC map used
GOM_TRA_1PNPDE20041208_202148_000000392032_00429_14511_0012.N1	DC map used
GOM_TRA_1PNPDE20041208_202334_000000492032_00429_14511_0013.N1	DC map used
GOM_TRA_1PNPDE20041208_202539_000000402032_00429_14511_0014.N1	DC map used
GOM_TRA_1PNPDE20041208_202908_000000972032_00429_14511_0015.N1	DC map used
GOM_TRA_1PNPDE20041208_203255_000000392032_00429_14511_0016.N1	DC map used
GOM_TRA_1PNPDE20041208_203739_000000362032_00429_14511_0017.N1	DC map used
GOM_TRA_1PNPDE20041209_205920_000000522032_00444_14526_0000.N1	DC map used
GOM_TRA_1PNPDE20041209_210150_000000602032_00444_14526_0001.N1	DC map used
GOM_TRA_1PNPDE20041209_210516_000000652032_00444_14526_0002.N1	DC map used
GOM_TRA_1PNPDE20041209_210713_000000672032_00444_14526_0003.N1	DC map used
GOM_TRA_1PNPDE20041209_211038_000000842032_00444_14526_0004.N1	DC map used
GOM_TRA_1PNPDE20041209_211359_000000542032_00444_14526_0005.N1	DC map used
GOM_TRA_1PNPDE20041209_211630_000000542032_00444_14526_0006.N1	DC map used
GOM_TRA_1PNPDE20041209_211858_000000542032_00444_14526_0007.N1	DC map used
GOM_TRA_1PNPDE20041209_212132_000000572032_00444_14526_0008.N1	DC map used
GOM_TRA_1PNPDE20041209_212331_000000382032_00444_14526_0009.N1	DC map used
GOM_TRA_1PNPDE20041209_212545_000000382032_00444_14526_0010.N1	DC map used
GOM_TRA_1PNPDE20041209_212727_000000392032_00444_14526_0011.N1	DC map used
GOM_TRA_1PNPDE20041209_212930_000000392032_00444_14526_0012.N1	DC map used
GOM_TRA_1PNPDE20041209_213108_000000452032_00444_14526_0013.N1	DC map used
GOM_TRA_1PNPDE20041209_213443_000000392032_00444_14526_0014.N1	DC map used
GOM_TRA_1PNPDE20041209_213728_000000942032_00444_14526_0015.N1	DC map used
GOM_TRA_1PNPDE20041217_200823_000000482033_00057_14640_0000.N1	DC map used
GOM_TRA_1PNPDE20041217_201112_000000532033_00057_14640_0001.N1	DC map used
GOM_TRA_1PNPDE20041217_201423_000000532033_00057_14640_0002.N1	DC map used

GOM_TRA_1PNPDE20041217_201606_000000562033_00057_14640_0003.N1	DC map used
GOM_TRA_1PNPDE20041217_201905_000000672033_00057_14640_0004.N1	DC map used
GOM_TRA_1PNPDE20041217_202218_000000522033_00057_14640_0005.N1	DC map used
GOM_TRA_1PNPDE20041217_202430_000000512033_00057_14640_0006.N1	DC map used
GOM_TRA_1PNPDE20041217_202732_000000582033_00057_14640_0007.N1	DC map used
GOM_TRA_1PNPDE20041217_202936_000000492033_00057_14640_0008.N1	DC map used
GOM_TRA_1PNPDE20041217_203151_000000372033_00057_14640_0009.N1	DC map used
GOM_TRA_1PNPDE20041217_203359_000000372033_00057_14640_0010.N1	DC map used
GOM_TRA_1PNPDE20041217_203616_000000372033_00057_14640_0011.N1	DC map used
GOM_TRA_1PNPDE20041223_041539_000000352033_00133_14716_0000.N1	DC map with no T dep.

In fig. 4.5-1 and 4.5-2 it is plotted the average DC inserted by the processor into the level 1b data products for the spectrometers SPA1 and SPB2 (per band: upper, central and lower). From the figures, it can be seen that the DC is increasing at the expected rate.

The same DC values are plotted in fig. 4.5-3 but for occultations belonging only to the reporting month.

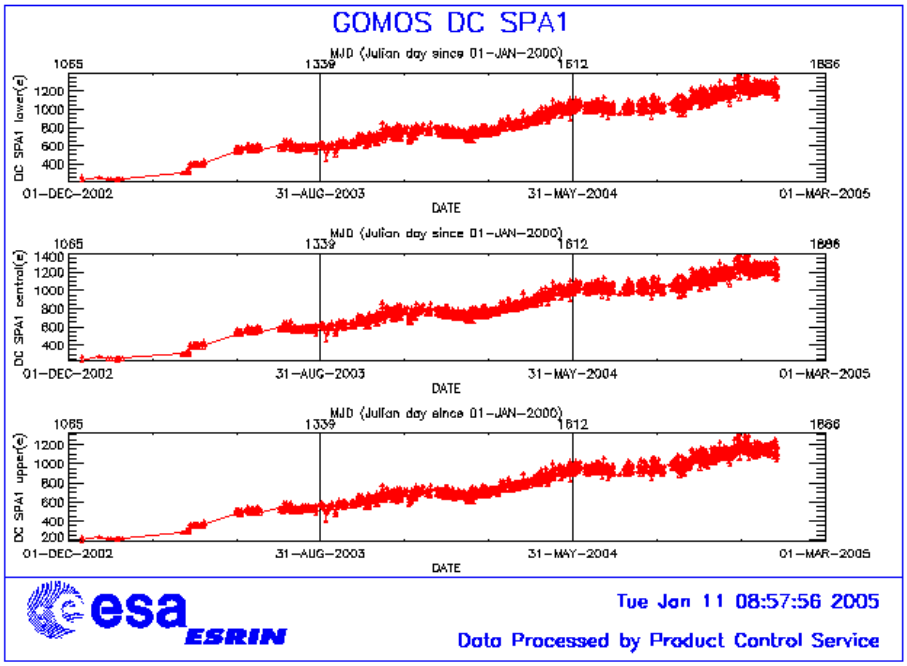

Figure 4.5-1: Mean DC evolution on SPA1 since 15th December 2002 until the end of the reporting period

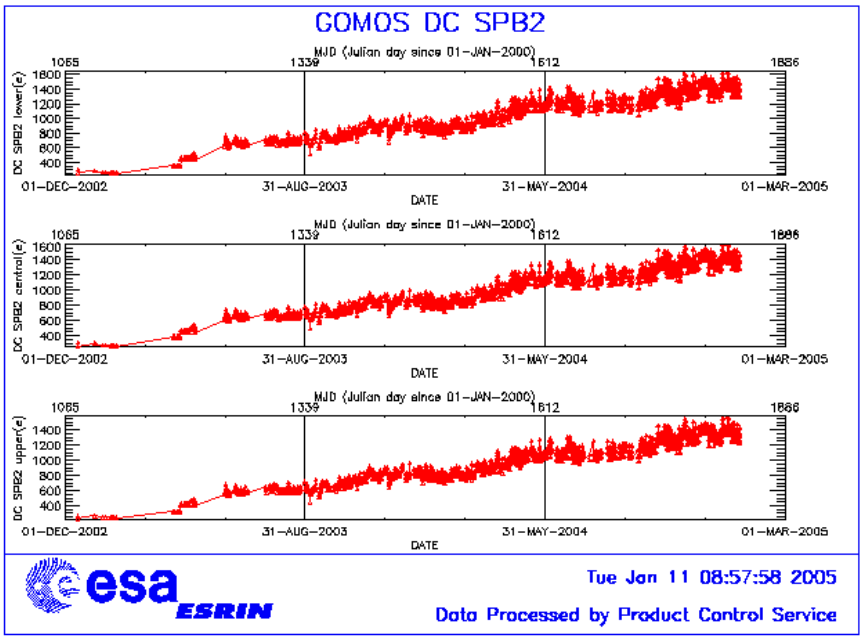

Figure 4.5-2: Mean DC evolution on SPB2 from 15th December 2002 until the end of the reporting period

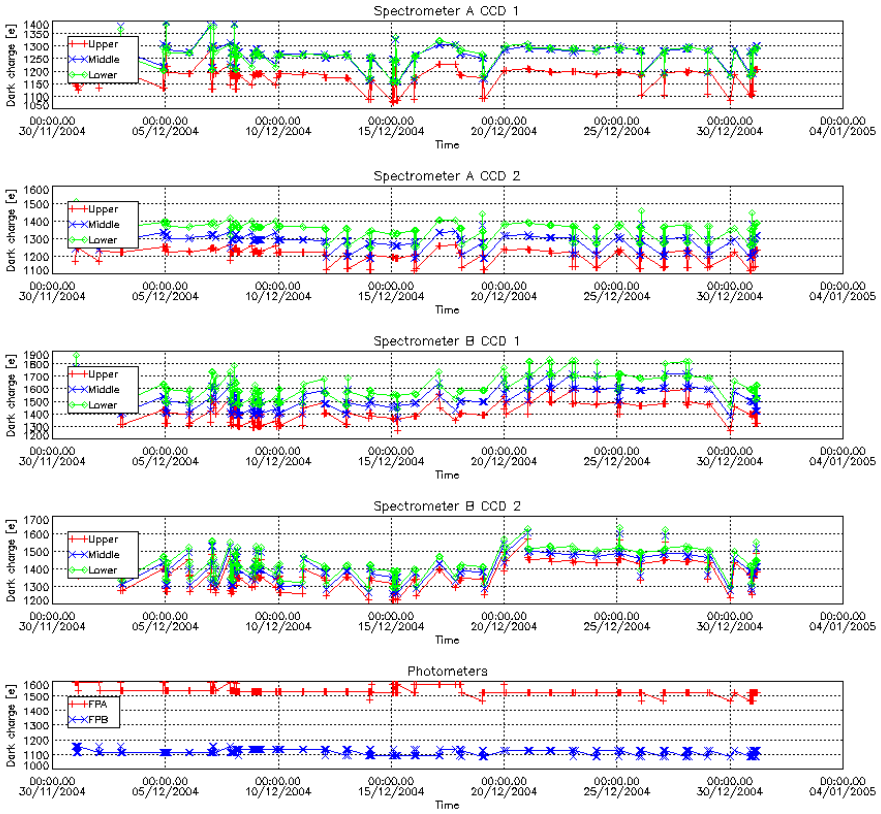

Figure 4.5-3: Mean Dark Charge of spectrometers and photometers during reporting period

4.5.2 SIGNAL MODULATION

A parasitic signal was found to be systematically present, added to the useful signal, at least for spectrometers A1 and A2. The modulation is corrected in the data processing, but the modulation signal standard deviation is routinely monitored in order to detect any trend (fig. 4.5-4).

The modulation standard deviation, for every spectrometer, is characterised as follows:

$$\sigma_{mod} = (\text{'static noises'} - \text{'total static variance'})^{1/2} / \text{gain} \qquad \text{(in ADU)}$$

- The 'static noises' are calculated from the DSA observation performed once per orbit
- The 'total static variance' is obtained from ADF data (electronic chain noise, quantization noise).

The standard deviation of the modulation signal (fig. 4.5-4) presents high values after the inclusion, at the end of March 2004, of the ESRIN level 0 data. It is now confirmed that the South Atlantic Anomaly is the cause of these unexpected peaks. The quality of ESRIN data, in particular over the SAA zone, is thus under investigation. However, in the second half of October the peaks are smaller because the DSA zone where the data are taking for this analysis is moving towards the Northern Hemisphere. At the end of October the DSA zone is definitely chosen by the planning system in the Northern Hemisphere (to fill the criteria 'DSA in full dark limb conditions') and the high peaks have disappeared.

It is also a very small decreasing trend observed, mainly for SPA1, which for now is not a reason to worry about.

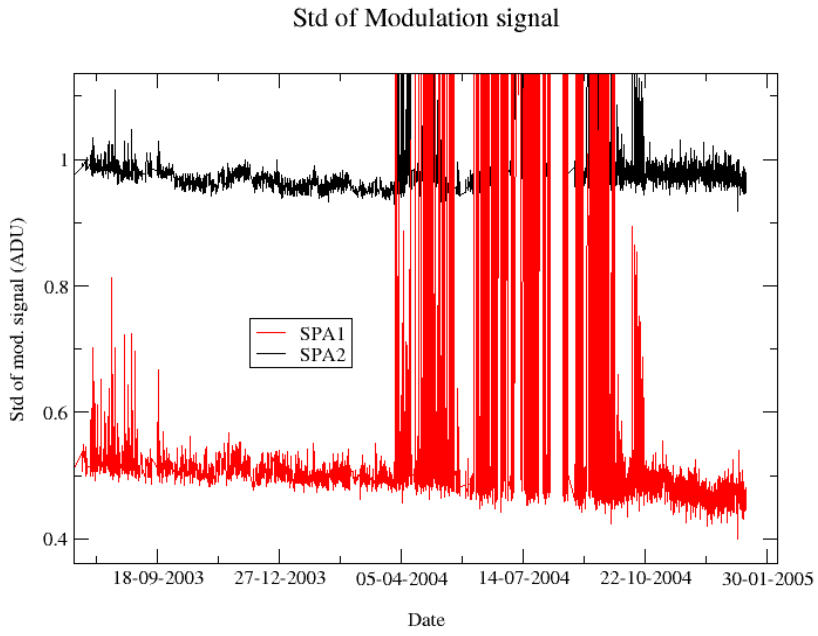

Figure 4.5-4: Standard deviation of the modulation signal

4.5.3 ELECTRONIC CHAIN GAIN AND OFFSET

No new electronic chain gain and offset calibration has been done during the reporting period so these results have been already presented in previous MR.

The routine monitoring of the ADC offset is a good indicator of the ageing of the instrument electronics. During the definition of this routine activity, an exercise has been done to analyze the variation of the ADC offset using the calibration observation in linearity mode (orbits 2810, 4384, 4834, 5219 and 5734). The fig. 4.5-5 presents the evolution of the calibrated ADC offset for each spectrometer electronic chain. The unexpected increase of this offset seems to be due to an external contribution. In the ADC offset calibration procedure, linearity observations are used with two integration times of 0.25 and 0.50 seconds to extrapolate to an integration time of 0 seconds that give the complete chain offset and not only the ADC offset. The complete offset contains any possible offsets, and especially the static dark charge (i.e. the dark charge that does not depend on the spectrometer integration time). If the memory area of the CCD is affected by the generation of hot pixels (this is confirmed by the presence of vertical lines visible in the measurement maps in spatial spread monitoring mode), it becomes that the increase observed in fig. 4.5-5 is due to these new hot pixels.

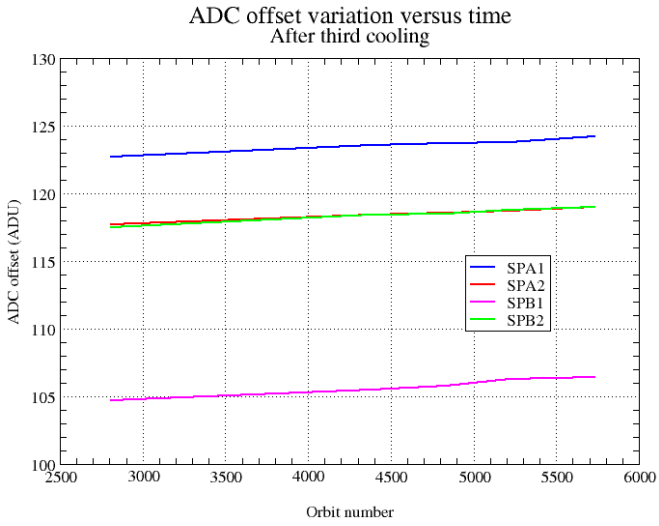

Figure 4.5-5: Evolution of the ADC offset for each spectrometer electronic chain

Next task consists in completing the analysis to confirm that the offset increase is due to the hot pixels in memory area. This can be proven by the study of the noise due to the increased dark charge. The increase of ADC offset will be assumed to be equal to the increase of 'static dark charge' and the corresponding noise will be computed and compared to the increase of the signal variance residual.

If we keep the ADC offset constant, as it is also used to compute the dark charge at band level used to correct the samples in the level 1b processing, the increase of the static dark charge - not taken into account in the ADC offset - is compensated by an artificial increase of the calibrated dark charge. So, the star and limb spectra are correctly corrected for dark charge. A small bias can be added to the instrument noise due to the incorrect dark charge level. Anyway, this quantity is not large enough to require a modification of the ADC offset value.

4.6 Acquisition, Detection and Pointing Performance

4.6.1 SATU NOISE EQUIVALENT ANGLE

The Star Acquisition and Tracking Unit (SATU) noise equivalent angle (SATU NEA) consists of the statistical angular variation of the SATU data above the atmosphere. The mean of the standard deviation (STD over the 50 values per measurement) above 105 km are computed for every occultation, giving two values per occultation: one in the 'X' direction, one in the 'Y' direction. A mean value per day in every direction and limb is calculated and monitored in order to assess instrument performance in terms of star pointing. The thresholds are 2 and 3 micro radians in 'X' and 'Y' directions respectively. Before May 2003, data above 90 km have been considered (instead of 105 km) but from May 2003 on, data taken in the mesospheric oxygen layer (located around 100 km altitude) have been avoided because they could cause fluctuations on the SATU data. Also the products with errors (error flag set) are discarded from May 2003 onwards.

It can be seen in fig. 4-6.1 that the SATU NEA had some increase for 'Y' direction for both dark and bright limbs but still well below the thresholds.

The results for some occultations belonging to previous months (monthly averages) are presented in fig. 4.6-2, where no trend is visible so far.

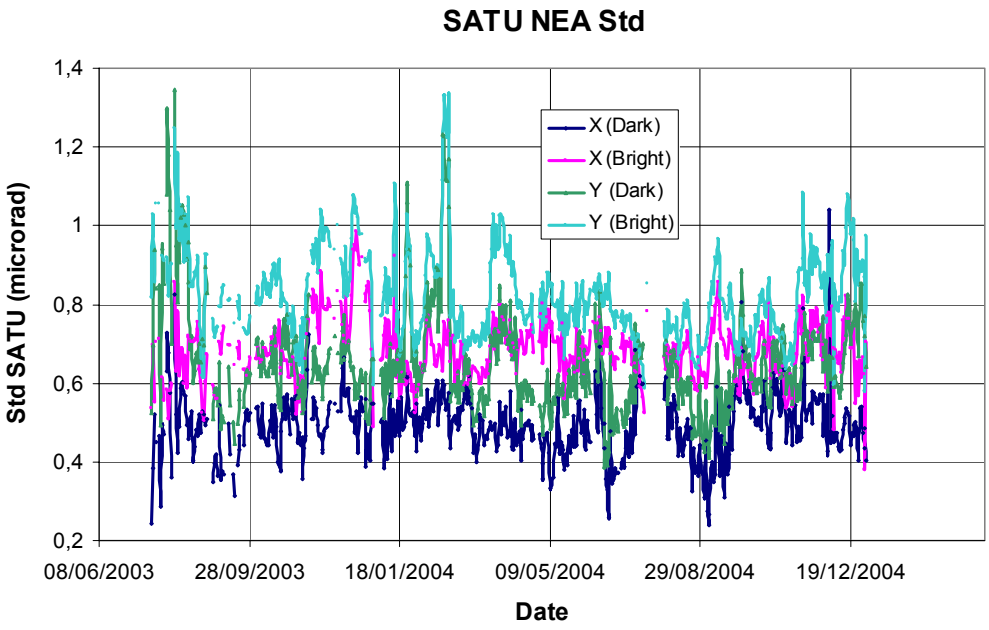

Thresholds:
'X' direction: 2 microrad
'Y' direction: 3 microrad

Figure 4.6-1: Average value per day of SATU NEA STD above 105 km

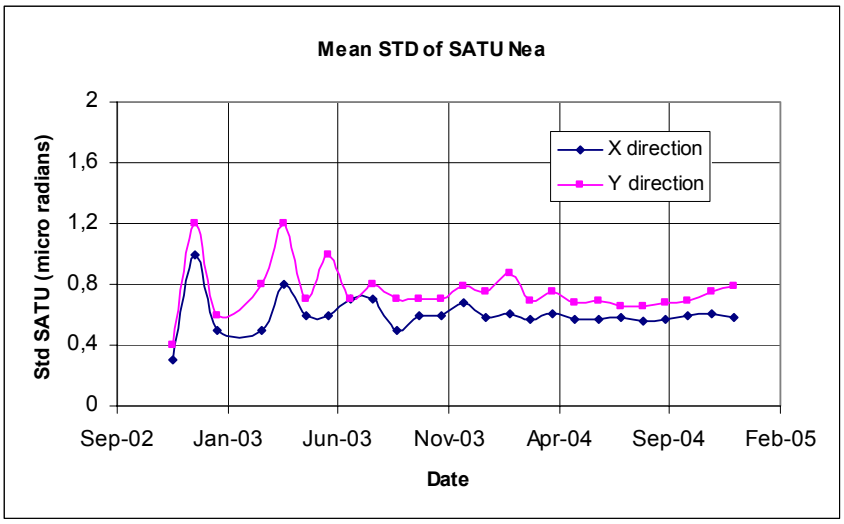

Figure 4.6-2: Average value per month of SATU NEA STD above 105 km

4.6.2 TRACKING LOSS INFORMATION

This verification consists of the monitoring of the tangent altitude at which the star is lost. It is an indicator of the pointing performance although it is to be considered that star tracking is also lost due to the presence of clouds and hence not only due to deficiencies in the pointing performance. Therefore, only the detection of any systematic long-term trend is the main purpose of this monitoring. The recent results are presented in fig. 4.6-3, 4.6-4 and 4.6-5:

- The dependence of the altitude at which tracking is lost on the magnitude of the star is very small because the tracking is mainly lost due to the refraction and the scintillation that depend on the atmospheric conditions.
- There are no stars lost at very high altitude neither in dark (fig. 4.6-3) nor in bright/twilight limbs (fig. 4.6-4 & 4.6-5).
- Some daily statistics are given in fig. 4.6-6 since October 2003. The high peaks are due to the long lasting occultations or partial occultations (occultations at the end of the orbit, being the entire occultation included within the following orbit). A decreasing trend is detected for the reporting period probably caused by the fact that there were neither long lasting occultations nor partial occultations within the level 1b dataset used for the monitoring.
- Some monthly statistics are given in fig. 4.6-7 calculated for a set of data and not for the whole months. A decreasing trend is observed for the monthly mean bright tangent altitude lost (see previous bullet).

Tangent altitude at which the star is lost

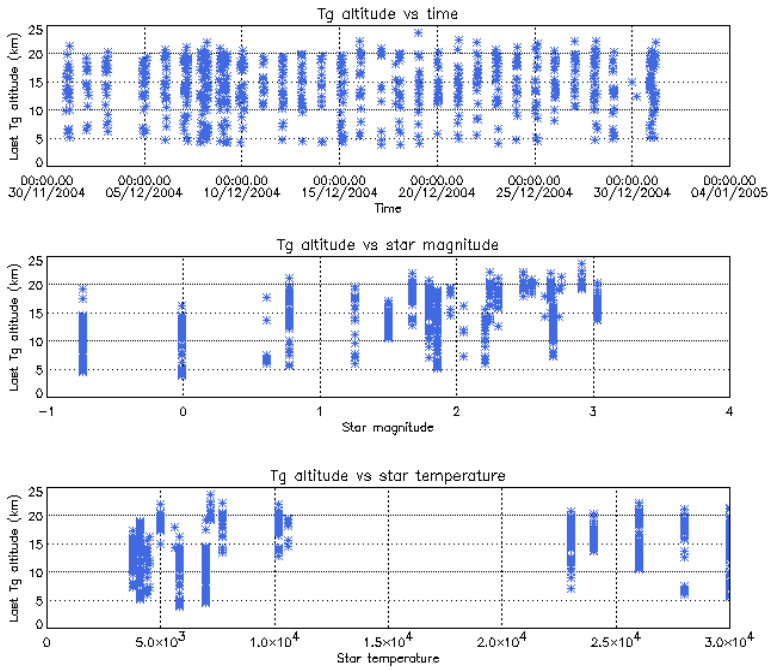

Figure 4.6-3: Last tangent altitude of the occultation (dark limb), point at which the star is lost

Tangent altitude at which the star is lost

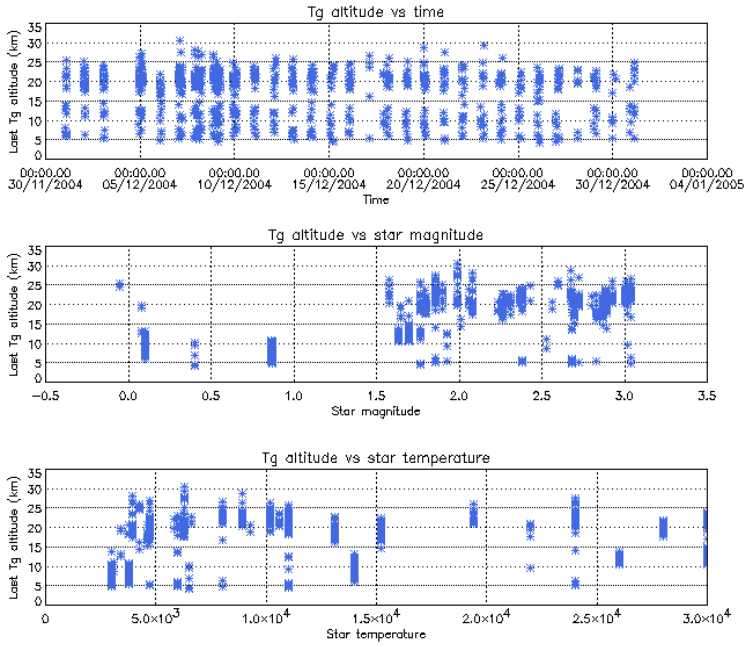

Figure 4.6-4: Last tangent altitude of the occultation (bright limb), point at which the star is lost

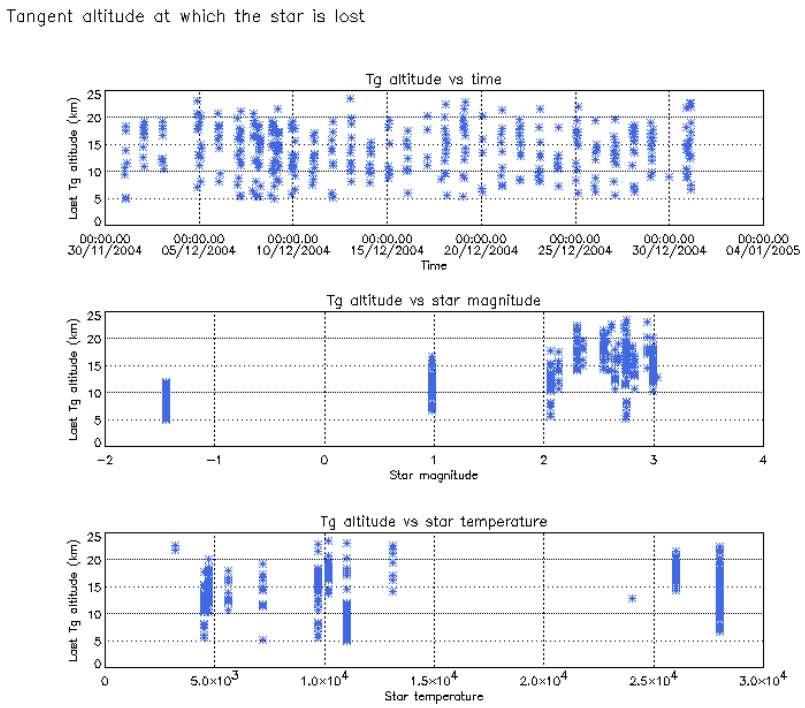

Figure 4.6-5: Last tangent altitude of the occultation (twilight limb), point at which the star is lost

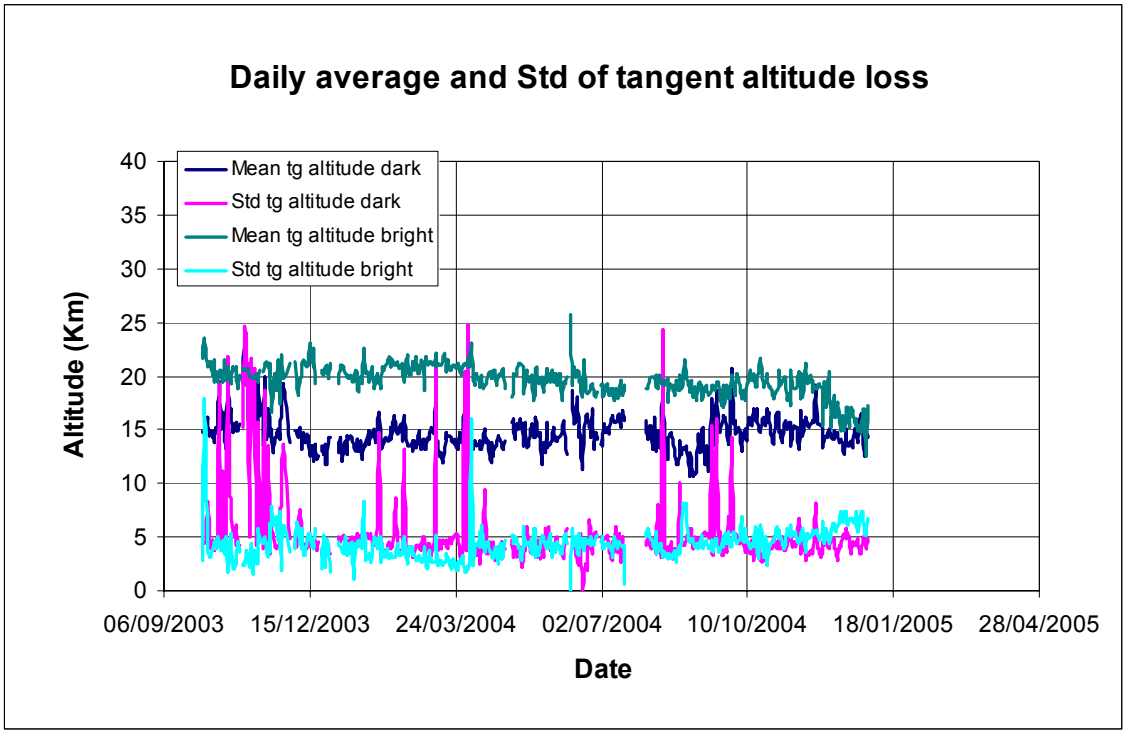

Figure 4.6-6: Daily average and STD of tangent altitude loss for the reporting period

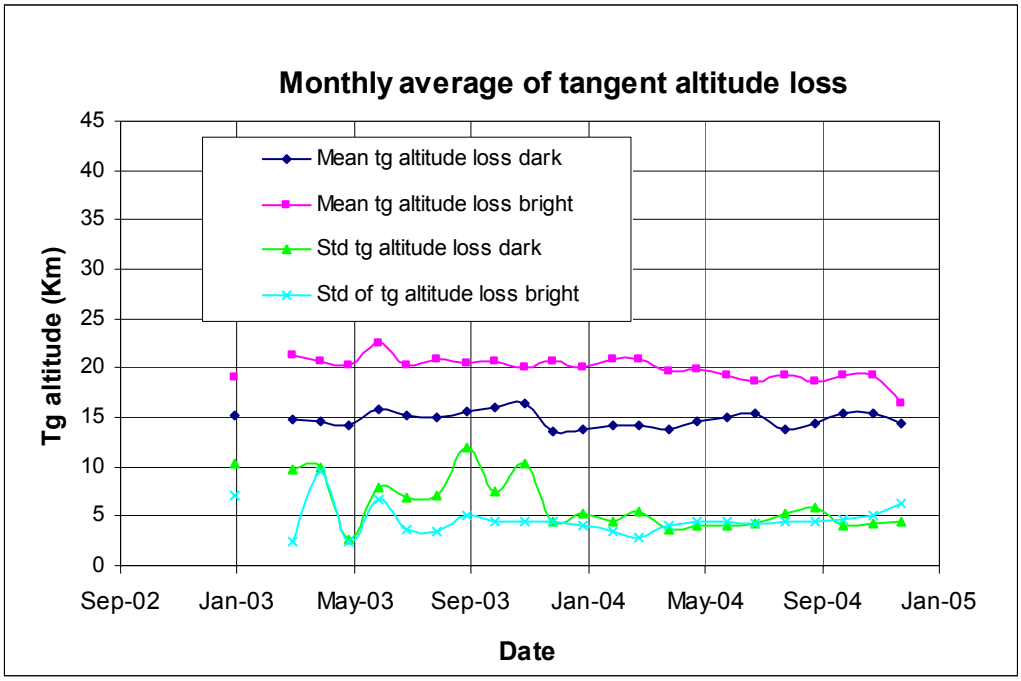

Figure 4.6-7: Monthly mean tangent altitude (and STD) at which the star is lost since January 2003

4.6.3 MOST ILLUMINATED PIXEL (MIP)

The MIP (Most Illuminated Pixel) is the star position on the SATU CCD in detection mode and it is recorded in the housekeeping data. The nominal centre of the SATU is pixel number **145** in elevation and number **205** in azimuth. The detection of the stars should not be far from this centre. All MIP values for one orbit every two days were extracted, averaged and plotted (fig. 4.6-8) until orbit 13472 (27th September 2004). After that orbit, and due to the importance of MIP data to monitor the ENVISAT pointing, every orbit is used to extract the MIP values. In order to be more accurate, only values of the MIP when GOMOS was in "DETECTION" pointing sub-mode are used.

As can be seen in fig. 4.6-8 the azimuth is always well within the threshold (table 4.6-1) since September 2002 even if a small variation is present. The elevation MIP has a significant variation (see the *note* below) till 12th December 2003 when a new PSO algorithm was activated in order to reduce the deviations of the ENVISAT platform attitude with respect to the nominal one. The annual amplitude of the MIP displacement is decreased from 18-20 pixels to 8-10 that means an important improvement of the ENVISAT pointing performance. This result confirms that, until now, the algorithm is working as expected. The MIP displacement will continue to be carefully monitored during the remaining mission.

Note: A MIP variation onto the SATU CCD of 50 pixels corresponds to a de-pointing of 0.1 degrees

Table 4.6-1: MIP Thresholds

MIP X	**Mean delta Az**	[198 - 210]
	Std delta Az	7
MIP Y	**Mean delta El**	[140 – 150]
	Std delta El	4

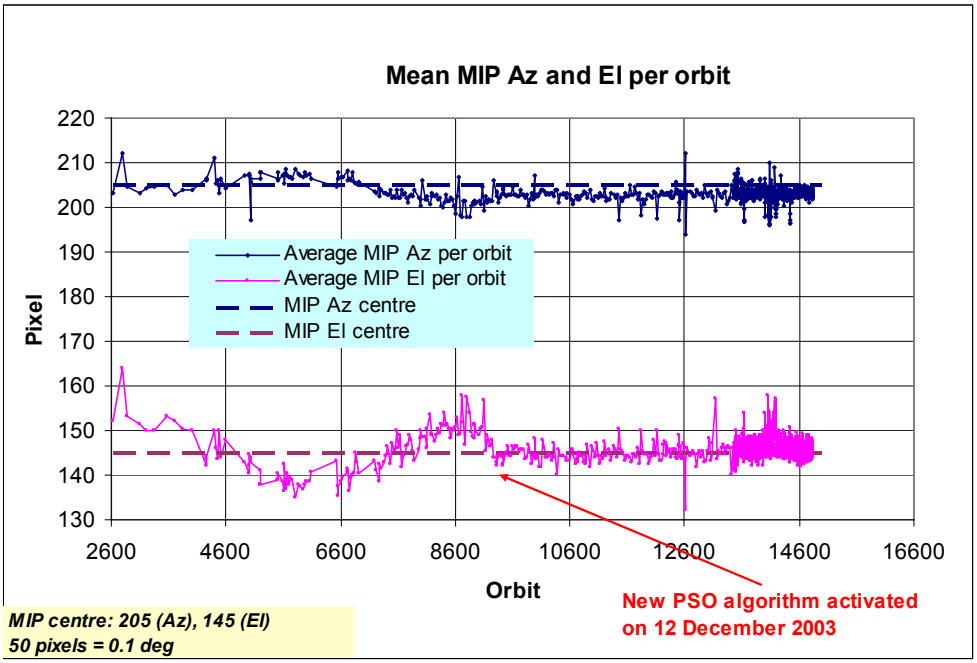

Figure 4.6-8: Mean values of MIP for some orbits since 1st September 2002 (see table 4.6-1)

Fig. 4.6-9 shows the standard deviation of azimuth and elevation that should be within the thresholds of table 4.6-1. Before orbit 13472 (all MIP values used for the average), the peaks mainly occur because data when no detection was performed, were also used for the average and STD calculation. The peaks observed after orbit 13472 mean that one (or more) star/s where detected very far from the SATU centre and, in this case, the star is lost during the centering phase (see section 3.2 for stars lost in centering).

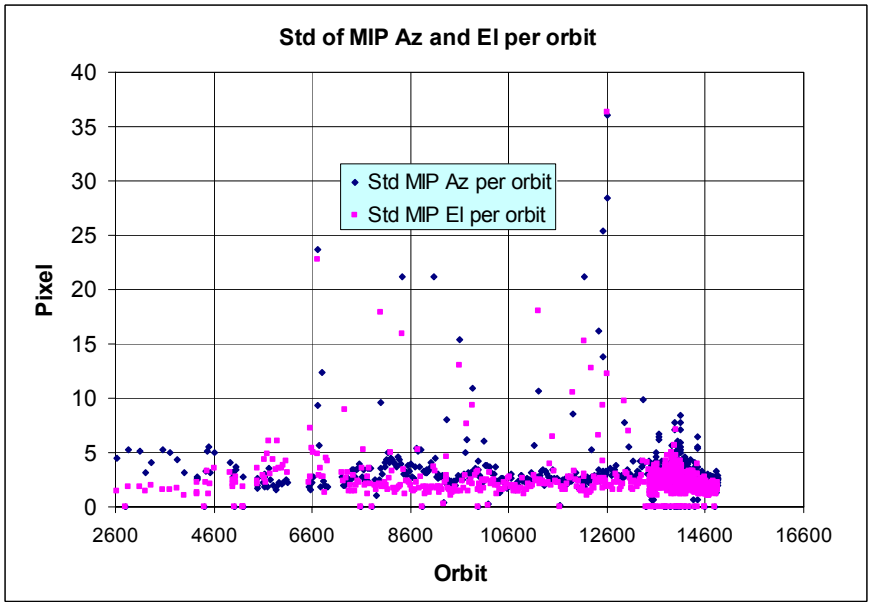

Figure 4.6-9: Standard deviation of MIP Azimuth and Elevation for some orbits since 1st September 2002 until end of reporting period (see table 4.6-1)

5 LEVEL 1 PRODUCT QUALITY MONITORING

5.1 Processor Configuration

5.1.1 VERSION

About 16% of GOM_TRA_1P products have been received in the PCF for routine quality control and long term trend quality monitoring. The current level 1-processor software version for the operational ground segment is GOMOS/4.02 (see table 5.1-1). The product specification is PO-RS-MDA-GS2009_10_3H. This processor has been cleared for initial level 1 data release, with a disclaimer for known artefacts (http://envisat.esa.int/dataproducts/availability/disclaimers) that are currently being resolved and will be implemented in the next release (http://envisat.esa.int/dataproducts/availability).

ESA is also providing 2003 products that are reprocessed with the prototype processor GOPR 6.0a. See table 5.1-2 for prototype level 1b versions and modifications.

Table 5.1-1: PDS level 1b product version and main modifications implemented

Date	Version	Description of changes
23-MAR-2004	Level 1b version 4.02 at PDHS-E and PDHS-K	Algorithm baseline level 1b DPM 6.0 • Adding a new calibration parameters (these values are hard coded at the moment) • Removal of redundancy chain from code • Modifications in the processing to apply new configuration and calibration parameter • New algorithm to determine between dark, twilight and bright limb and to handle data accordingly • Added handling of source packages with invalid packet header • Added enumerations for all configuration flags • See ref. [2] for more details
31-MAY-2003	Level 1b version 4.00 at PDHS-E and PDHS-K	Algorithm baseline level 1b DPM 5.4: • Modulation correction step added after the cosmic rays detection processing • Inversion of the non-linearity and offset corrections • Modification of the computation of the estimated background signal measured by the photometers: use the spectrometer radiometric sensitivity curve and the photometer transfer function. • Use of the dark charge map at orbit level computed from the DSA (dark sky area) if any in the level 0 product • Implementation of a new unfolding algorithm for the photometer samples • See ref. [2] for more details
21-NOV-2002	Level 1b version 3.61 at PDHS-E and PDHS-K	Algorithm baseline DPM 5.3: • Review of some default values • New definition of one PCD flag (atmosphere) • Temporal interpolation of ECMWF data • See ref. [2] for more details

Table 5.1-2: GOPR level 1b product version and main modifications implemented

Date	Version	Description of changes
17-MAR-2004	GOPR 6.0a	• Provide SFA and SATU angles in degrees • Elevation angle dependency of the reflectivity LUT added in the algorithms • Ratio upper/star signal added (FLAGUC) • Add Dark Charge used for dark charge correction (per band) • Flag for illumination condition (PCDillum) • Minimum sample value for which the cosmic rays detection processing is applied (Crmin) is a function of gain index • Logic for computation of the flags attached to the reference star spectrum (Flref) modified • Add the computation of the sun direction in the inertial geocentric frame to be written in the level 1b and limb products. • Spectrometer effective sampling time added (To be completed)
25-JUL-2003	GOPR 5.4f	• The demodulation process is applied only in full dark limb and twilight limb conditions.
17-JUL-2003	GOPR 5.4e	• Sun zenith angle is computed in the geolocation process. The occultation is now classified into (0) full dark limb condition, (1) bright limb condition and (2) twilight limb condition. • No background correction applied in full dark limb condition. The location of the image of the star spectrum on the CCD array is no more aligned with the CCD lines.
02-JUL2003	GOPR 5.4d	• The maximum number of measurements is set to 509 (instead of 510) in the GOPR prototype.
17-MAR-2003	GOPR 5.4c	• Modification of the CAL ADFs (update of the limb radiometric LUT). The products are affected only if the limb spectra are converted into physical units • Modifications to allow compatibility with ACRI computational cluster (no modifications of the results) • Modification of the logic to handle dark charge map refresh at orbit level (DSA data is now directly processed by the level 1b processor if available in the level 0 product). No impact on the results
21-FEB-2003	GOPR 5.4b	• DC map values are rounded when written in the level 1b product • Modification of the CAL ADFs (update of the wavelength assignment of SPB1 and SPB2) • Modify the computation of flag_mod in the modulation correction routine
17-JAN-2003	GOPR 5.4a	• use the start and stop dates of the occultation when calling the CFI interpol instead of start and stop dates of the level 0 product • modify the ECMWF filename information in the SPH of the level 1b and limb products

5.1.2 AUXILIARY DATA FILES (ADF)

The ADF's files in tables 5.1-3, 5.1-4, 5.1-5, 5.1-6 and 5.1-7 have been disseminated to the PDS during the whole mission. For every type of file, the validity runs from the start validity time until the start validity time of the following one, but if an ADF file has been disseminated after the start validity time, it is obvious that it will be used by the PDHS-E and PDHS-K PDS only after the dissemination time (this happens the majority of the times). As the other ADF's, the calibration auxiliary file (GOM_CAL_AX) has been updated several times in the past (table 5.1-7) but the difference is that now it is updated in a

weekly basis with only new DC maps, and that is why the files used in December are reported in a separate table (table 5.1-8) that will change from month to month. On 7th, 13th and 17th December new calibration ADF's were disseminated with updated DC maps of orbits 14480, 14565 and 14622 respectively (table 5.1-8). Note that the files outlined in yellow are the set of auxiliary files used during the reporting period.

Table 5.1-3: Table of historic GOM_PR1_AX files used by PDS for level 1b products generation

Used by PDS for Level 1b products generation in period	GOM_PR1_AX (GOMOS processing level 1b configuration file)
01-MAR-2002 → 29-MAR-2002	**GOM_PR1_AXVIEC20020121_165314_20020101_000000_20200101_000000** • Pre-launch configuration
30-MAR-2002 → 14-NOV-2002	**GOM_PR1_AXVIEC20020329_115921_20020324_200000_20100101_000000** • Changed num_grid_upper, thr_conv and max_iter in the atmospheric GADS
Not used	**GOM_PR1_AXVIEC20020729_083756_20020301_000000_20100101_000000** • Cosmic Ray mode + threshold • DC correction based on maps • Non-linearity correction disabled
Not used	**GOM_PR1_AXVIEC20021112_170331_20020301_000000_20100101_000000** • Central background estimation by linear interpolation + associated thresholds
15-NOV-2002 → 26-MAR-2003	**GOM_PR1_AXVIEC20021114_153119_20020324_000000_20100101_000000** • Same content as GOM_PR1_AXVIEC20021112_170331_20020301_000000_20100101_000000 but validity start updated so as to supersede according to the PDS file selection rules GOM_PR1_AXVIEC20020329_115921_20020324_200000_20100101_000000
27-MAR-2003 → 19-MAR-2004	**GOM_PR1_AXVIEC20030326_085805_20020324_200000_20100101_000000** • Same content as GOM_PR1_AXVIEC20021112_170331_20020301_000000_20100101_000000 but validity start updated so as to supersede according to the PDS file selection rules GOM_PR1_AXVIEC20020329_115921_20020324_200000_20100101_000000
20-MAR-2004 → 22-MAR-2004	**GOM_PR1_AXVIEC20040319_134932_20020324_200000_20100101_000000** • Ray tracing parameter changed: convergence criteria set to 0.1 microrad
23-MAR-2004 → 01-APR-2004 *Notes*: • This file was constructed from GOM_PR1_AXVIEC20030326_085805_20020324_200000_20100101_000000 (so without the ray tracing parameter changed) • This file was used by the GOMOS/4.02 processors before the IECF dissemination. The dissemination was done on 25th March 2004	**GOM_PR1_AXVIEC20040316_144850_20020324_200000_20100101_000000** GOM_PR1 ADF for version GOMOS/4.02, changes: • The central band estimation mode • Atmosphere thickness • Altitude discretisation

02-APR-2004	**GOM_PR1_AXVIEC20040401_083133_20020324_200000_20100101_000000** • Ray tracing parameter changed: convergence criteria set to 0.1 microrad

Table 5.1-4: Table of historic GOM_INS_AX files used by PDS for level 1b products generation

Used by PDS for Level 1b products generation in period	GOM_INS_AX (GOMOS instrument characteristics file)
01-MAR-2002 → 29-JUL-2002	**GOM_INS_AXVIEC20020121_165107_20020101_000000_20200101_000000** • Pre-launch configuration
30-JUL-2002 → 12-NOV-2002	**GOM_INS_AXVIEC20020729_083625_20020301_000000_20100101_000000** • Factors for the conversion of the SFA angles from SFM axes to GOMOS axes
13-NOV-2002 → 16-JUL-2003	**GOM_INS_AXVIEC20021112_170146_20020301_000000_20100101_000000** • No more invalid spectral range
Not used	**GOM_INS_AXVIEC20030716_080112_20030711_120000_20100101_000000** • New value for SFM elevation zero offset for redundant chain: 10004
17-JUL-2003	**GOM_INS_AXVIEC20030716_105425_20030716_120000_20100101_000000** • Bias induct azimuth redundant value set to -0.0084 rad (-0.4813 deg)

Table 5.1-5: Table of historic GOM_CAT_AX files used by PDS for level 1b products generation

Used by PDS for Level 1b products generation in period	GOM_CAT_AX (GOMOS Stat Catalogue file)
01-MAR-2002	**GOM_CAT_AXVIEC20020121_161009_20020101_000000_20200101_000000** • Pre-launch configuration

Table 5.1-6: Table of historic GOM_STS_AX files used by PDS for level 1b products generation

Used by PDS for Level 1b products generation in period	GOM_STS_AX (GOMOS Star Spectra file)
01-MAR-2002	**GOM_STS_AXVIEC20020121_165822_20020101_000000_20200101_000000** • Pre-launch configuration

Table 5.1-7: Table of historic GOM_CAL_AX files used by PDS for level 1b products generation

Used by PDS for Level 1b products generation in period	GOM_CAL_AX (GOMOS Calibration file)
01-MAR-2002 → 29-JUL-2002	**GOM_CAL_AXVIEC20020121_164808_20020101_000000_20200101_000000** • Pre-launch configuration
Not used	**GOM_CAL_AXVIEC20020121_142519_20020101_000000_20200101_000000** • Pre-launch configuration
30-JUL-2002 → 12-NOV-2002	**GOM_CAL_AXVIEC20020729_082426_20020717_193500_20100101_000000** • Band setting information • Wavelength assignment • Spectral dispersion LUT • ADC offset for Spectrometers

	• PRNU maps • Thermistor coding LUT • DC maps
Not used	**GOM_CAL_AXVIEC20021112_165603_20020914_000000_20100101_000000** • Band setting information • DC maps • PRNU maps • Wavelength assignment • Spectral dispersion LUT • Radiometric sensitivity LUT (star and limb) • SP-FP intercalibration LUT • Vignetting LUT • Reflectivity LUT • ADC offset
13-NOV-2002 → 30-JAN-2003	**GOM_CAL_AXVIEC20021112_165948_20021019_000000_20100101_000000** • Only DC maps updated
31-JAN-2003 → 11-APR-2003	**GOM_CAL_AXVIEC20030130_133032_20030101_000000_20100101_000000** • Only DC maps updated (using DSA of orbit 04541)
12-APR-2003 → 02-JUN-2003	**GOM_CAL_AXVIEC20030411_065739_20030407_000000_20100101_000000** • Modification of the radiometric sensitivity curve for the limb spectra. Note that the modification of this LUT has no impact on the GOMOS processing. The LUT is just copied into the level 1b limb product for user conversion purpose. • Updated DC map only (using DSA of orbit 05762).
03-JUN-2003: from this date onwards, mainly updates to DC maps are done. Every month, the table of new GOM_CAL files with **only** DC maps updated is provided (table 5.1-8). Eventual changes to this file not corresponding only to DC maps updates will be reported in this table.	**GOM_CAL_AXVIEC20030602_094748_20030531_000000_20100101_000000** • Updated DC maps only (using DSA of orbit 06530)
13-FEB-2004 → 23-FEB-2004	**GOM_CAL_AXVIEC20040212_103916_20040209_000000_20100101_000000** • Update of the reflectivity LUT • Updated DC maps (Orbit 10194, date 11-FEB-2004)

Table 5.1-8: Calibration ADF for reporting period. These files are updated (only with DC maps) in a 8-10 days basis

Used by PDS for Level 1b products generation in period	GOM_CAL_AX (GOMOS Calibration file)
30-NOV-2004 → 06-DEC-2004	**GOM_CAL_AXVIEC20041129_135000_20041127_000000_20100101_000000** (orbit 14365, date 28-NOV-2004)
08-DEC- 2004 → 13-DEC-2004	**GOM_CAL_AXVIEC20041207_081221_20041205_000000_20100101_000000** (orbit 14480, date 06-DEC-2004)
14-DEC- 2004 → 17-DEC-2004	**GOM_CAL_AXVIEC20041213_094740_20041211_000000_20100101_000000** (orbit 14565, date 12-DEC-2004)
18-DEC- 2004 → 10-JAN-2005	**GOM_CAL_AXVIEC20041217_142407_20041216_000000_20100101_000000** (orbit 14622, date 16-DEC-2004)

5.2 Quality Flags Monitoring

In this section it is monitored some Product Quality information stored in level 1b products that did not have a fatal error (MPH error flag not set). The products with fatal errors were around 1% of the products received during December for the quality monitoring.

On the one hand, for every product we have information of the **number of measurements** where a given problem was detected (i.e. number of invalid measurements, number of measurements containing saturated samples, number of measurements with demodulation flag set…). On the other hand, there are **flags** that indicate problems within the product (i.e. flag set to one if the reference spectrum was computed from DB, flag set to zero if SATU data were not used…).

For the information on the number of measurements a plot of percentages with respect to time is provided in fig. 5.2-1. Part of this information, the most relevant one, is also plotted in a world map as a function of ENVISAT position: % of cosmic ray hits per profile, % of datation errors per profile, % of star falling outside the central band per profile and % of saturation errors per profile (fig.5-2.2).

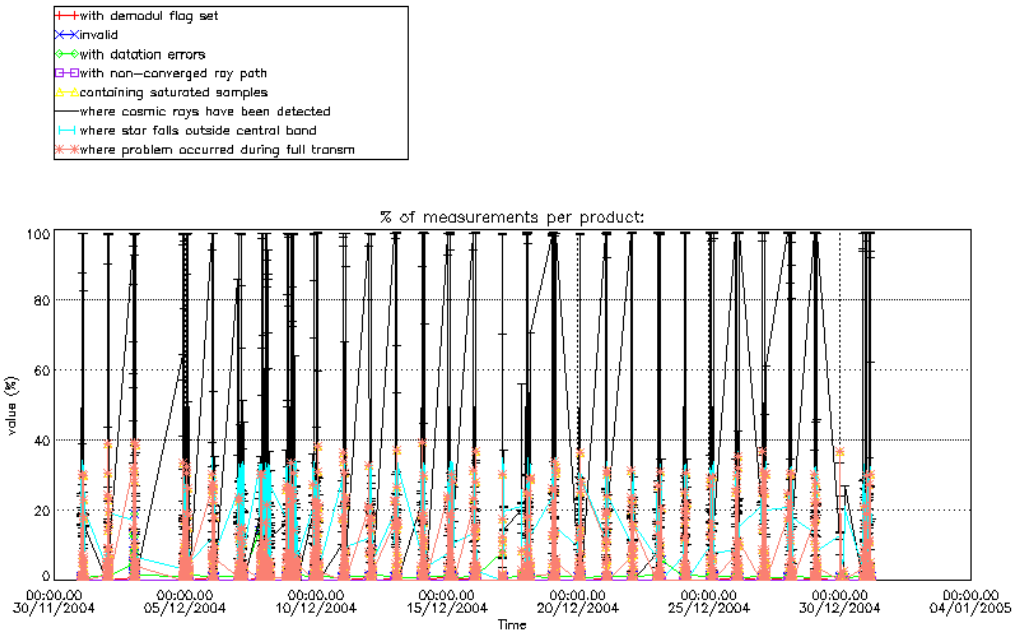

Figure 5.2-1: Level 1b product quality monitoring with respect to time

It can be seen from fig. 5.2-1 that the cosmic rays hits occurred several times for the 95% of the measurements of the products. Looking at fig. 5.2-2 it can be clearly observed that this high percentage occurred when the satellite crossed the South Atlantic Anomaly (SAA) zone. Also the percentage of saturation errors per profile increased over SAA zone.

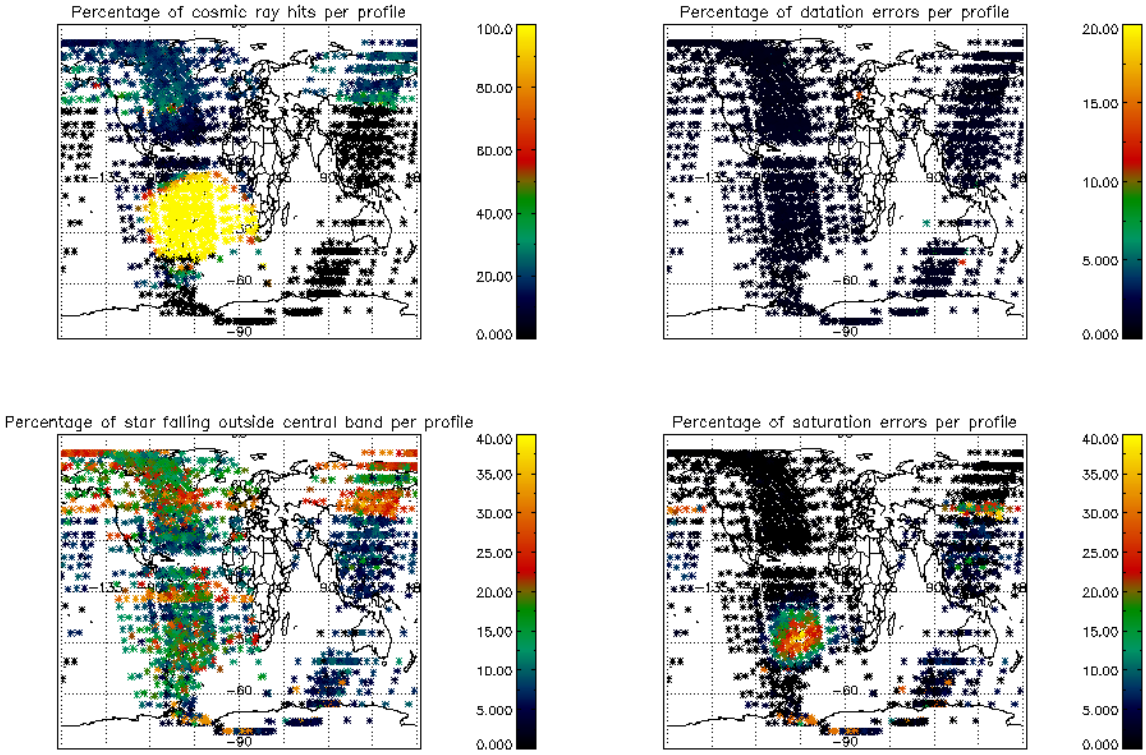

Figure 5.2-2: Level 1b product quality monitoring with respect to geolocation of ENVISAT

Another observation from fig. 5.2-1 is that, for many products, the 25 % of the measurements have the star signal falling outside the central band. In fig. 5.2-2 it is observed that this percentage occurred mainly during the ascending part of the orbit (night-side of the orbit) while in the descending part (day-side of the orbit) the percentage is around 10 %. This is because during the night the stars are lost deeper within the atmosphere and the turbulence phenomena become more important, producing the star to be less 'focused' on the spectrometers central band. The other values (% of invalid measurements per product, % of measurements per product with datation errors…) are quite low.

The flag information is given in table 5.2-1. It is reported also the percentage of the products that have at least one measurement with demodulation flag set.

Table 5.2-1: Percentage of products during the reporting period with:

At least one measurement with demodulation flag set:	14.2406 %
Reference spectrum computed from DB:	0.00000 %
Reference spectrum with small number of measurements:	0.00000 %
SATU data not used:	0.00000 %

5.2.1 QUALITY FLAGS MONITORING (EXTRACTED FROM LEVEL 2 PRODUCTS)

In this section it is plotted the Product Quality information coming from the level 1 processing that is stored also in the level 2 products. Only products that did not have a fatal error (MPH error flag not set) are considered. The purpose of using the level 2 data is simply that the percentage of level 2 products arriving in PCF for the quality monitoring is much higher. For December, 97.5% of the archived products have been received. The plots are very similar to fig. 5.2-1 and 5.2-2 (demodulation flag information is not included) but separating ascending from descending passes. The ascending part of the orbit (above -60^{o} latitude) is in dark limb while the descending (below 43 ^{o} latitude) is in bright limb.

Fig. 5.2-3 and 5.2-4 present some quality information as a function of the time whereas in fig. 5.2-5 and 5.2-6 the plot is respect to the satellite position at the beginning of the occultations. In ascending (fig. 5.2-5) the SAA is perfectly localized by the high percentage of cosmic ray hits per product (upper left panel). It is not the same if we look fig. 5.2-6, because in descending the most of the occultations are in bright limb conditions and the cosmic rays detection processing is not activated.

Another clear difference between ascending and descending is that in ascending (fig. 5.2-3) the percentage of measurements "where a problem occurred during the full transmission" per product is around 2% while for the descending passes is much higher. This is due to the saturation that occurs mainly in bright limb. In ascending the saturation occurs over the SAA zone but it is quite low elsewhere.

There are some products with a high percentage of invalid measurements and measurements with datation errors. These products are mainly partial occultations: the last occultation of a level 0 product; being the entire occultation included in the following level 0 file. These products have a degraded quality and should not be used by the users.

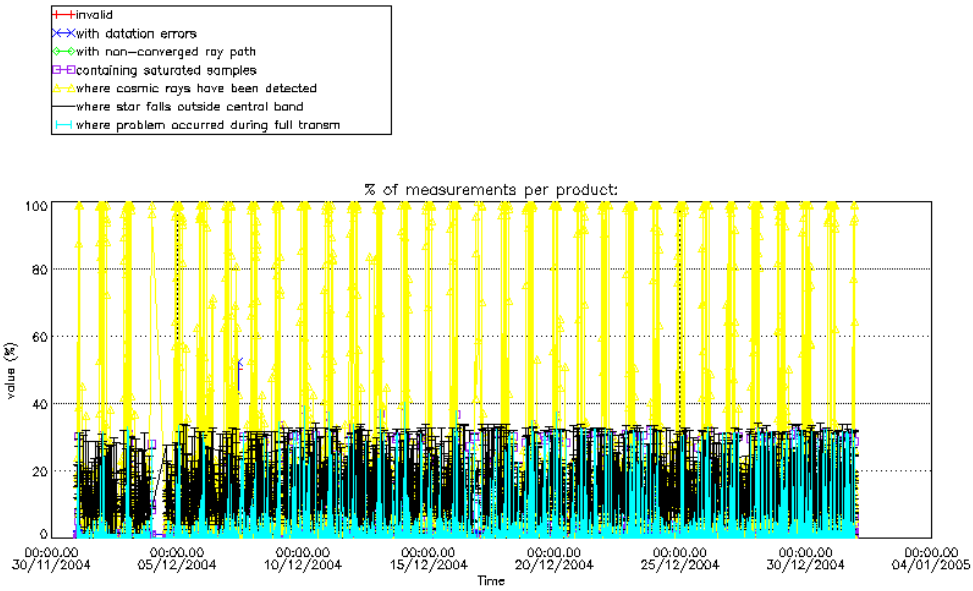

Figure 5.2-3: Level 1b product quality monitoring with respect to time ASCENDING ENVISAT passes

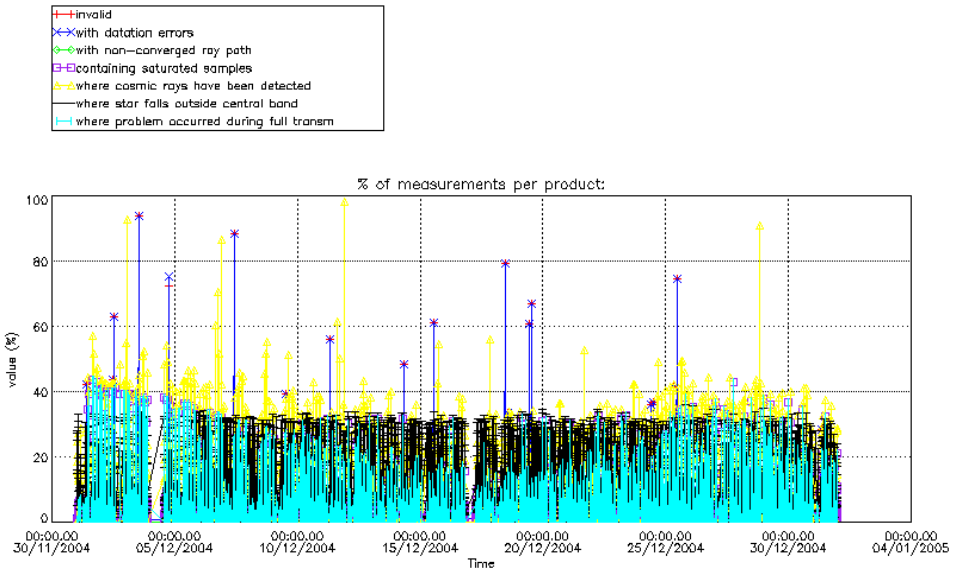

Figure 5.2-4: Level 1b product quality monitoring with respect to time <u>DESCENDING</u> ENVISAT passes

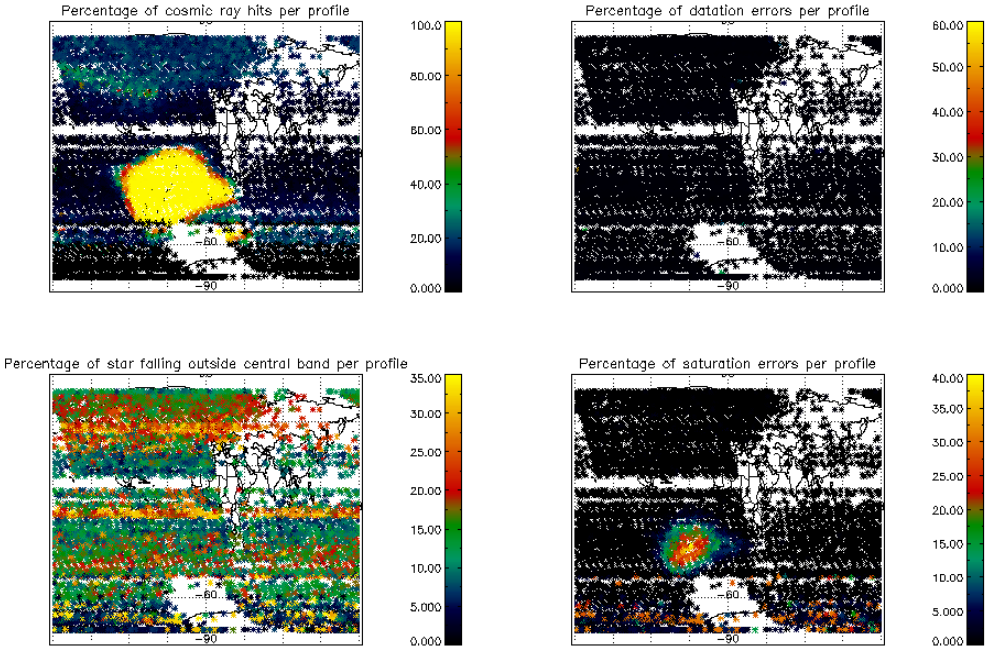

Figure 5.2-5: Level 1b product quality monitoring with respect to geolocation for <u>ASCENDING</u> ENVISAT passes

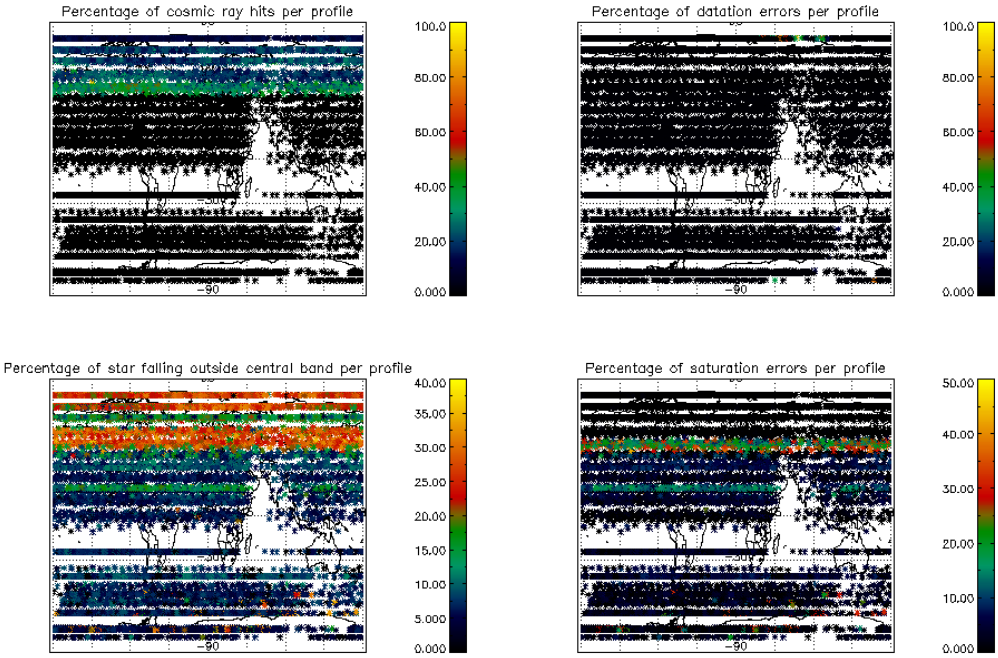

Figure 5.2-6: Level 1b product quality monitoring with respect to geolocation for DESCENDING ENVISAT passes

5.3 Spectral Performance

A new spectral calibration has been performed during the reporting period. As occurred during previous calibrations, the results reach the warning values.

The values reported (table 5.3-1) are, for every star ID (1, 2, 4, 9, 18, 25), the wavelength of the first useful pixel of SPA2. This value is calculated by addition to the actual wavelength assignment, the spectral shift for which a maximum correlation has been found between the reference spectrum and the one of the occultation.

During the last wavelength calibration analysis performed using two occultations, the spectral shifts were -0.098 for star id number 2 and -0.1 for star id number 1 (see table 5.3-1). These shifts are greater than 0.07 (warning value) and QWG investigations that have been initiated already in March 2004 will continue.

The star number 4 is left in table 5.3-1 even if the values of the wavelength are very different from the nominal one. It should be just kept in mind that the values of the shift should be always of the same order (~0.4) but this star will not be used for calibration purposes.

Table 5.3-1: Wavelength assignment calculated for several occultations since November 2002

Star ID / Level 0 date	1	2	4	9	18	25
20021112_062935	Occ.30: 690.455750	Occ.26: 690.458740		Occ.28: 690.492981		
20021219_102754		Occ.33: 690.468140	Occ.26: 690.875122			
20030101_151630	Occ.3: 690.445068	Occ.37: 690.466003	Occ.30: 690.878540			
20030110_121504		Occ.32: 690.465088	Occ.25: 690.882385			
20030201_090221						Occ.21: 690.492981
20030415_123156			Occ.29: 690.959534		Occ.20: 690.552002	Occ.28: 690.492981
20030419_170041			Occ.29: 690.957520		Occ.23: 690.555420	
20030428_072600					Occ.19: 690.553645	Occ.28: 690. 492981
20030717_053233				Occ. 22: 690.473816	Occ. 26: 690.446594	
20040123_091615	Occ.1: 690.400513 Occ.40: 690.401550	Occ.35: 690.415161	Occ.27: 690.852478			
20040222_065917			Occ.25: 690. 850830			Occ.21: 690. 492981
20040128_163559	Occ.3: 690.399414					Occ.23: 690. 492981
20040804_123934	Occ.20 690.411377	Occ.24 690.404724		Occ.25 690.397522	Occ.29 690.397156	
20041101_074131	Occ. 26 690.403748	Occ. 21 690.392700		Occ. 24 690.398254		
20050101_014125	Occ.18 690.386841	Occ.14 690.394348	Occ. 6: 690.811157			

5.4 Radiometric Performance

5.4.1 RADIOMETRIC SENSITIVITY

The monitoring performed consists in the calculation of the radiometric sensitivity of each CCD by computing the ratio between parts of the reference spectrum using specific stars. The parts of spectrum used are:

- UV: 250–300 nm
- Yellow: 500–550 nm
- Red: 640–690 nm
- Ir1: 761-770 nm
- Ir2: 935-944 nm

For the spectrometers the ratios are with respect to the 'yellow' spectral range. For the photometers, the ratio is calculated dividing the mean photometer signal above the atmosphere (115 km) by the 'yellow' spectral range (for PH1) or by the 'red' spectral range (for PH2).

The variation of the ratio should be within a given threshold actually set to 10% (see table 5.4-1 that corresponds to fig. 5.4-1). For every star, this variation is calculated as the difference between the maximum (or minimum) ratio, and the mean over the 15 first values (if there are not 15 values computed yet, all values are used).

Table 5.4-1: Variation of RS for the different ratios (corresponds to fig. 5.4-1). Should be less than 10%

Star Id	% Variation of UV ratio	% Variation of Red ratio	% Variation of IR1 ratio	% Variation of IR2 ratio	% Variation of Ph1 ratio	% Variation of Ph2 ratio
1	2.04276	0.511867	0.401701	0.217333	30.8640	70.2278
2	0.416756	0.652793	0.625175	0.216532	4.52068	7.93166
4	0.150048	0.838286	1.52463	1.24313	8.08780	23.5227
9	4.63446	0.416139	0.783493	0.466555	835.855	2624.41
18	0.990748	0.681692	0.844914	0.852089	1865.10	5139.44
25	10.6943	0.699922	0.654513	1.12662	28.0870	147.396

Values outside the warning threshold set to 10% are observed mainly for the photometers, and investigations were performed by the QWG. An inaccurate reflectivity correction LUT was suspected to be the cause of the increase but a new one is in use since 12th February 2004 and the results did not change.

In fig. 5.4-2 the two fast photometer ratios have been splinted by stars, so one plot per star is presented. As it can be seen, for star id 9 only two points are the cause of the big variation of the percentage while for star id 18 it is just one point. This means that there is not a real problem in the radiometric sensitivity for the photometers even if the outliers exist and an explanation should be found. For star id 25, the problem is different. It is observed a real variation of the ratios but as it is only seen for this star, it can be concluded that the variation should be linked to the star itself and not to the photometers.

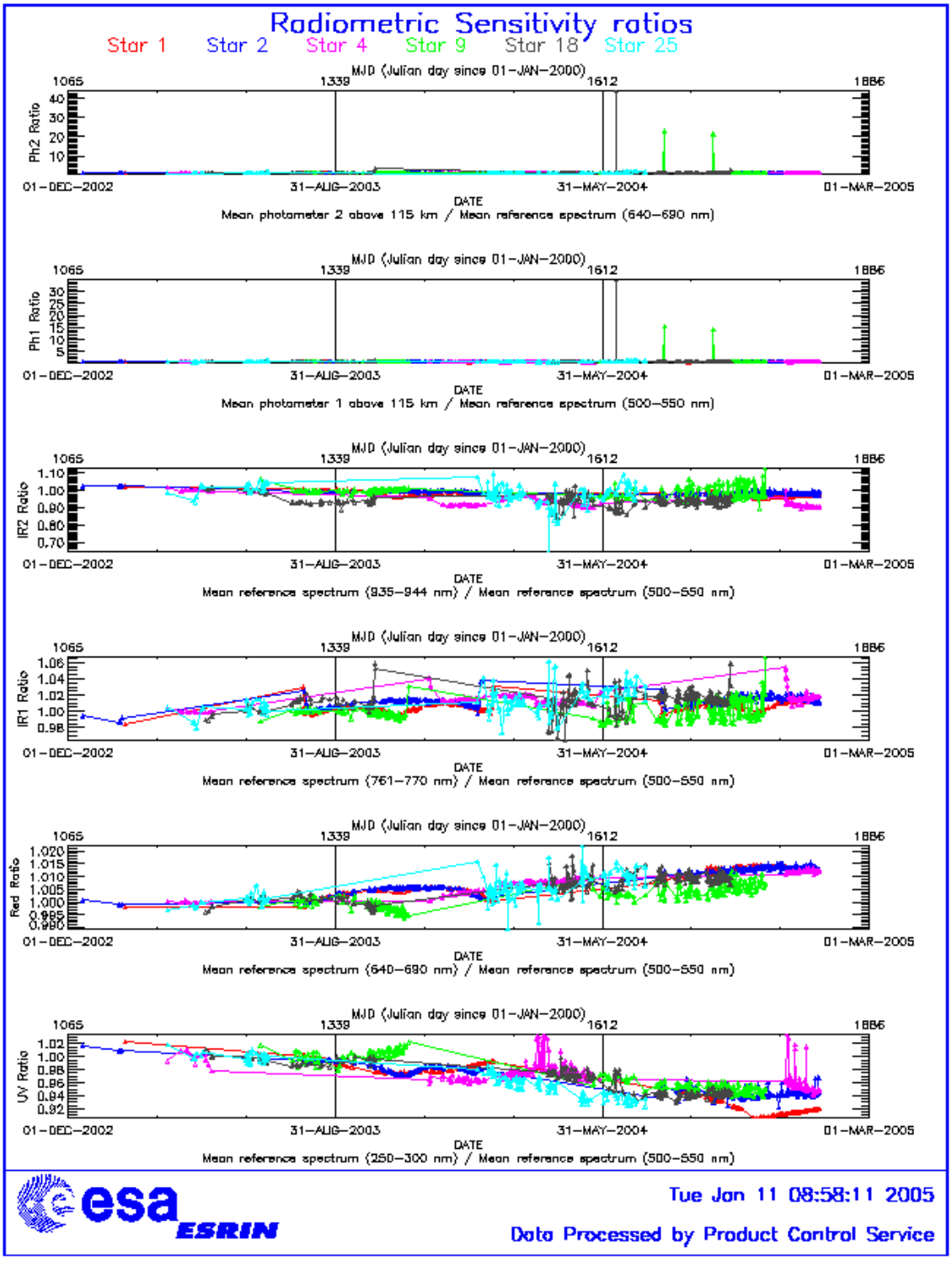

Figure 5.4-1: Radiometric sensitivity ratios since December 2002

For star 25 also the UV ratio is greater than 10%. Looking at fig. 5.4-1, it is clear that there is a global decrease of UV ratios for all the stars. This confirms the expected degradation suffered by the UV optics that is, anyway, very small considering also the small variation for the rest of the stars (table 5.4-1).

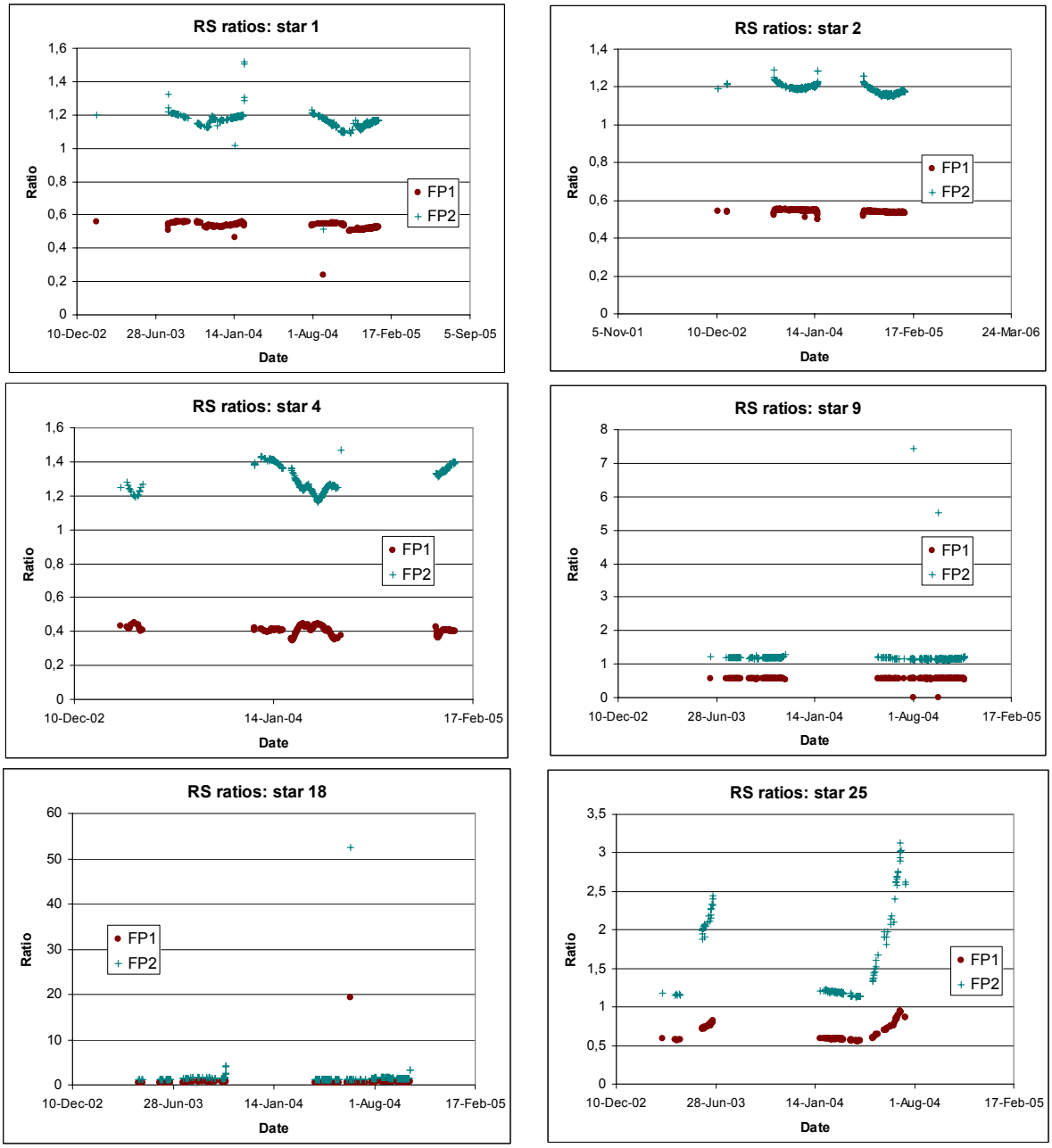

Figure 5.4-2: Fast Photometer ratios for the different monitoring stars. They are the same ratios plotted in fig. 5.4-1 (the ones corresponding to PH1 and PH2) but now one plot per star.

5.4.2 PIXEL RESPONSE NON UNIFORMITY

No new PRNU calibration has been performed during the reporting period. This means that the PRNU maps inside the ADF remain as they are without any change for the moment.

5.5 Other Calibration Results

Future reports will address other calibration results, when available.

6 LEVEL 2 PRODUCT QUALITY MONITORING

6.1 Processor Configuration

6.1.1 VERSION

Level 2 products from the operational ground segment have been disseminated during December to the users. About 97.5% of the archived GOM_NL__2P products have been received in the PCF for routine quality control and long term trend monitoring. The current level 2-processor software version for the operational ground segment is GOMOS/4.02 (see table 6.1-1). The product specification is PO-RS-MDA-GS2009_10_3H. The improvements defined at the first Validation Workshop have been implemented into the prototype processor GOPR 6.0a (see table 6.1-2), before implementation into the operational one. In the mean time, Cal/Val teams are supplied with selected data sets generated by this prototype processor (version also used for the GOMOS reprocessing, see section 6.1.3).

Table 6.1-1: PDS level 2 product version and main modifications implemented

Date	Version	Description of changes
23-MAR-2003	Level 2 version 4.02 at PDHS-E and PDHS-K	Algorithm baseline level 2 DPM 5.5: Section 3 • Add references to technical notes on Tikhonov regularization • Change High level breakdown of modules: SMO/PFG • Change parameter: NFS in l2 ADF • Change parameter σ_G in l2 ADF (Table 3.4.1.1-II) • Change content of Level 2/res products - GAP • Change time sampling discretisation • Add covariance matrix explanation Section 5 • Replace SMO by PFG VER-1/2: Depending on NFS, Apply either a Gaussian filter or a Tikhonov regularization to the vertical inversion matrix • Unit conversion applied on kernel matrix

		• Suppress VER-3 Section 6 • GOMOS Atmospheric Profile (GAP): not used in this version • Time sampling in equation (6.5.3.7-73) • See ref. [3] for more details
31-MAY-2003	Level 2 version 4.00 at PDHS-E and PDHS-K	Algorithm baseline level 2 DPM 5.4: • Revision of some default values • Add a new parameter • Transmission model computation: suppress tests on valid pixels and species • Apply a Gaussian filter to the vertical inversion matrix • Very low signal values are substituted by threshold value • See ref. [3] for more details
21-NOV-2002	Level 2 version 3.61 at PDHS-E and PDHS-K	Algorithm baseline level 2 DPM 5.3a: • Revision of some default values • Wording of test T11 • Dilution term computation of jend • Covariance computation scaling applied before and after • See ref. [3] for more details

Table 6.1-2: GOPR level 2 product version and main modifications implemented

Date	Version	Description of changes
17-MAR-2004	GOPR 6.0a	• Rename Turbulence MDS into High Resolution Temperature MDS (HRTP) • Add vertical resolution per species in local densities MDS • Add Solar zenith angle at tangent point and at satellite level in geolocation ADS • Add "tangent point density from external model" in geolocation ADS • Suppress contribution of "tangent point density from external model" in "local air density from GOMOS atmospheric profile" in geolocation ADS (to be completed)
18-AUG-2003	GOPR 5.4d	• Tikhonov regularisation is implemented
18-MAR-2003	GOPR 5.4b	• Modification to implement the computation of Tmodel for spectrometer B (in version 5.4b, the Tmodel for SPB is still set to 1)
30-JAN-2003	GOPR 5.4a	• Modifications for ACRI internal use only. No impact on level 2 products.

6.1.2 AUXILIARY DATA FILES (ADF)

The ADF's files in table 6.1-3 and 6.1-4 are used by the PDS to process the data from level 1 to level 2. For every type of file, the validity runs from the start validity time until the start validity time of the following one, but if an ADF file has been disseminated after the start validity time, it is obvious that it

will be used by the PDHS-E and PDHS-K PDS only after the dissemination time (this happens the majority of the times).

Table 6.1-3: Table of historic GOM_PR2_AX files used by PDS for level 2 products generation

Used by PDS for Level 2 products generation in period	GOM_PR2_AX (GOMOS Processing level 2 configuration file)
01-MAR-2002 → 29-JUL-2002	**GOM_PR2_AXVIEC20020121_165624_20020101_000000_20200101_000000** • Pre-launch configuration
30-JUL-2002 → 02-SEP-2002	**GOM_PR2_AXVIEC20020729_083851_20020301_000000_20100101_000000** • Maximum value of chi2 before a warning flag is raised (set to 5) • Maximum number of iterations for the main loop (set to 1)
03-SEP-2002 → 12-NOV-2003	**GOM_PR2_AXVIEC20020902_151029_20020301_000000_20100101_000000** • Maximum value of chi2 before a warning flag is raised (set to 100)
13-NOV-2003 → 22-MAR-2004	**GOM_PR2_AXVIEC20021112_170458_20020301_000000_20100101_000000** • Smoothing mode • Hanning filter • Number of iterations • Spectral windows to suppress the O2 absorption in the high spectral range of SPA2
23-MAR-2004 *Note*: this file was used by the GOMOS/4.02 processors before the IECF dissemination. The dissemination was done on 25th March 2004	**GOM_PR2_AXVIEC20040316_145613_20020301_000000_20100101_000000** • Pressure at the top of the atmosphere • Number of GOMOS sources data (used in GAP) • Activation flag for GOMOS sources data (GAP) • Smoothing mode (after the spectral inversion) • Atmosphere thickness

Table 6.1-4: Table of historic GOM_CRS_AX files used by PDS for level 2 products generation

Used by PDS for Level 2 products generation in period	GOM_CRS_AX (GOMOS Cross Sections file)
01-MAR-2002 → 08-MAR-2002	**GOM_CRS_AXVIEC20020121_164026_20020101_000000_20200101_000000** • Pre-launch configuration
09-MAR-2003 → 29-JUL-2002	**GOM_CRS_AXVIEC20020308_185417_20020101_000000_20200101_000000** • Corrected NUM_DSD in MPH - was 14 and is now 19 - and corrected spare DSD format by replacing last spare by carriage returns in file GOM_CRS_AXVIEC20020121_164026_20020101_000000_20200101_000000
30-JUL-2002 → 25-MAR-2004	**GOM_CRS_AXVIEC20020729_082931_20020301_000000_20100101_000000** • O3 cross-sections summary description (SPA) • NO3 cross-sections summary description • O2 transmissions summary description • H2O transmissions summary description • O3 cross sections (SPA)
26-MAR-2004 *Note*: the file was disseminated on 27 Jan 2004 but could not be used by PDS until version GOMOS/4.02 was in operation	**GOM_CRS_AXVIEC20040127_150241_20020301_000000_20100101_000000** • Update of the O2 and H2O transmissions (S.A input) • Extension by continuity of the O3 cross-section for SPB

6.1.3 RE-PROCESSING STATUS

To provide Cal/Val teams with early access to improved algorithms, selected occultations are processed with the prototype processor and made available to ACVT members. In addition, reprocessing of the full 2003 historic dataset has been performed with the prototype processor, and activities to complete the historic archive with the complete 2002 and 2004 dataset are underway. Data can be retrieved via web query from http://www.enviport.org/gomos/index.jsp. FTP access to bulk reprocessing results (one tar file of GOMOS products per day) is allowed from the D-PAC: ftp://gomo2usr@ftp-ops.de.envisat.esa.int.

The table 6.1-5 presents the status of the GOMOS reprocessing task in terms of availability of the instrument, level 0 input products and level 1b/2 output products. The status is presented by cycle. Each cycle is made of 501 orbits or 35 days. The last three columns of the table indicate the percentage of availability of each item with respect to the instrument availability in observation mode (i.e. for example without taking account the calibration or DSA observation of GOMOS).Values greater than 100% may occur due to the fact that some calibration observations are not taken into account in the instrument availability but they can be processed. See more details on http://www.fr-acri.com/gomval_web/news/board.htm

Table 6.1-5: Summary of reprocessing status at ACRI

Cycle	Orbits	Cycle Time Interval	% Instr. Availability	% L0 in ACRI	% Lv1b/L2 in ACRI
5	556-1056	08/04/02 21:59 - 13/05/02 20:18	89.6	0.0	0.0
6	1057-1557	13/05/02 21:59 -17/06/02 20:18	86.4	0.0	0.0
7	1558-2058	17/06/02 21:59 - 22/07/02 20:18	88.8	0.2	0.0
8	2059-2559	22/07/02 21:59 - 26/08/02 20:18	88.0	0.0	0.0
9	2560-3060	26/08/02 21:59 - 30/09/02 20:18	75.0	7.2	0.0
10	3061-3561	30/09/02 21:59 - 04/11/02 20:18	95.4	2.7	0.0
11	3562-4062	04/11/02 21:59 - 09/12/02 20:18	88.4	0.0	0.0
12	4063-4563	09/12/02 21:59 - 13/01/03 20:18	95.0	0.0	0.0
13	4564-5064	13/01/03 21:59 - 17/02/03 20:18	97.4	78.7	78.5
14	5065-5565	17/02/03 21:59 - 24/03/03 20:18	60.7	95.7	95.4
15	5566-6066	24/03/03 21:59 - 28/04/03 20:19	84.6	77.4	75.2
16	6067-6567	28/04/03 21:59 - 02/06/03 20:18	14.0	94.3	94.3
17	6568-7068	02/06/03 21:59 - 07/07/03 20:19	52.9	85.7	84.9
18	7069-7569	07/07/03 21:59 - 11/08/03 20:19	65.1	97.2	97.2
19	7570-8070	11/08/03 21:59 - 15/09/03 20:19	84.0	95.2	94.3
20	8071-8571	15/09/03 21:59 - 20/10/03 20:19	93.6	97.2	96.8
21	8572-9072	20/10/03 21:59 - 24/11/03 20:19	92.6	98.9	98.1
22	9073-9573	24/11/03 21:59 - 29/12/03 20:19	90.6	102.8	102.8
23	9574-10074	29/12/03 21:59 - 02/02/04 20:19	95.0	0.0	0.0
24	10075-10575	02/02/04 21:59 - 08/03/04 20:19	95.2	0.0	0.0
25	10576-11076	08/03/04 21:59 - 12/04/04 20:19	96.6	0.0	0.0
26	11077-11577	12/04/04 21:59 - 17/05/04 20:19	100.0	0.0	0.0
27	11578-12078	17/05/04 21:59 - 21/06/04 20:19	46.3	0.0	0.0
28	12079-12579	21/06/04 21:59 - 26/07/04 20:19	0.0	0.0	0.0
29	12580-13080	26/07/04 21:59 - 30/08/04 20:19	0.0	0.0	0.0

6.2 Quality Flags Monitoring

In this section it is plotted some information contained in the Quality Summary data set of level 2 products of December. In particular, it is depicted the percentage of flagged points per profile for the local species O_3, H_2O, NO_2 and Air. Only products in dark limb illumination conditions and without fatal errors (error flag in the MPH set to "0") are used.

A profile point in a level 2 product is flagged when:

- The local density is less than a given minimum value
- The local density is greater than a given maximum value
- A negative local density was found
- The line density is not valid. And it occurs when:
  - The acquisition from level 1b is not valid
  - There is no acquisition used for reference star spectrum
  - The line density is less than a given minimum value
  - The line density is greater than a given maximum value
  - A negative line density was found

  For species: air, aerosol, O_3, NO_2, NO_3, OClO
  - No convergence after a given number of LMA iterations
  - χ^2 out of LMA is bigger than χ^2
  - Failure of inversion

  For species: O_2, H_2O
  - Spectro B only: no convergence
  - Spectro B only: data not available
  - Spectro B only: covariance not available

Looking at the fig. 6.2-1 the most evident characteristic that can be observed is the high percentage of flagged points per profile for H_2O. Users should not use these data, as their quality is still poor. The percentage of flagged points per profile for O_3 and Air is around 35% whereas for NO_2 it becomes 60%.

The same information is plotted in fig. 6.2-2 as a function of the first tangent point of every profile. There are points mainly between -35^o and $+63^o$ latitude because in this period of the year full dark illumination condition occultations (only those products have been used for these plots) are found on that region. In summer, full dark illumination data are mainly in the Southern Hemisphere while in winter it is contrary: full dark illumination occultations will be found mainly in the Northern Hemisphere.

It can be seen that there are latitudinal bands with almost the same color (same percentages). This means that the percentages of flagged points per profile have a dependence on the stars that have been observed: a given star is always observed at the same latitude but at different longitude.

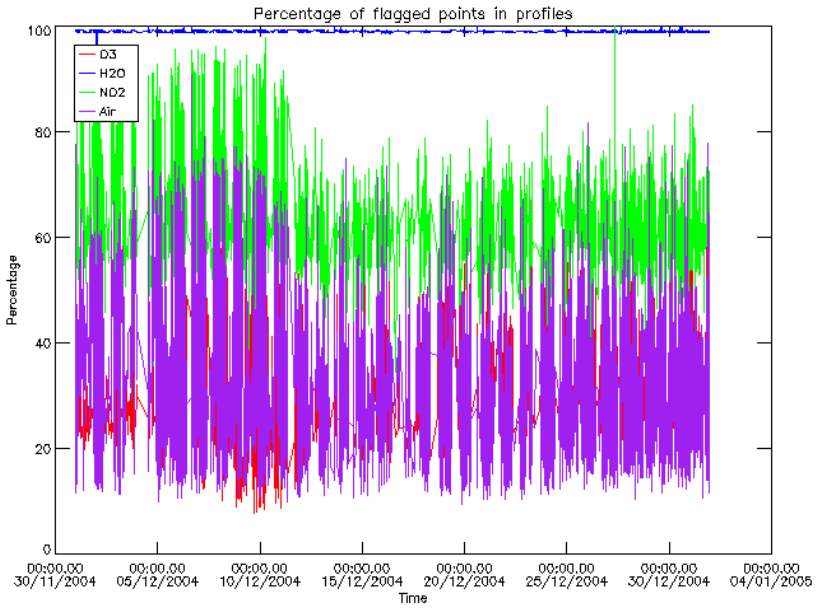

Figure 6.2-1: Percentage of flagged points per profile

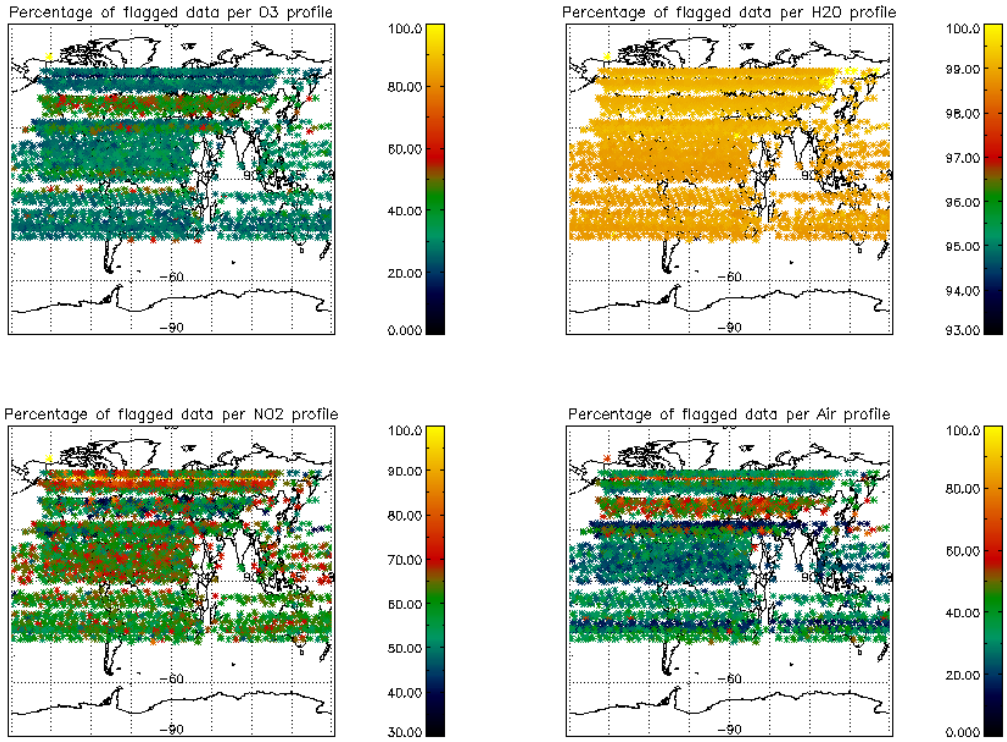

Figure 6.2-2: Percentage of flagged points per profile as a function of the first tangent point of the profile

6.3 Other Level 2 Performance Issues

6.3.1 MONTHLY AVERAGE OF O_3 PROFILES

The plot presented in fig. 6.3-1 is the average of the Ozone values during December in a grid of 0.5 degrees in latitude per 1 km in altitude. Occultations in dark limb illumination conditions and profile points that are not flagged have been used. Some known characteristics can be seen:

- O_3 concentrations show a decrease with latitude near 40 km altitude. In the lower latitudes O_3 is generated by photolysis of O_2
- In the middle stratosphere (25-30 km) O_3 is strongly influenced by transport effects. Strong meridional and zonal transport is visible in middle and higher latitudes
- The lower stratosphere shows an O_3 increase with latitude. Highest values can be found within the polar regions due to downward transport of rich air masses

However, other characteristics seem not to be realistic as some values below 15 km, where data are not reliable at the moment.

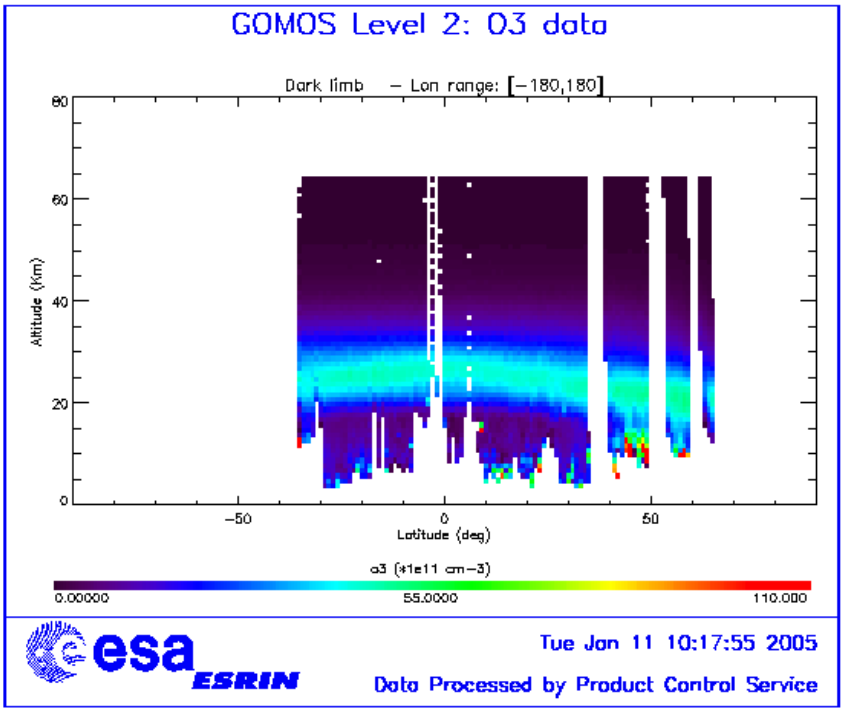

Figure 6.3-1: Average GOMOS O_3 profiles during December in a grid of 0.5° latitude x 1 km altitude

6.3.2 INFLUENCE OF STAR TEMPERATURE ON VERTICAL PROFILES (GOPR V6.0A)

6.3.2.1 Vertical profiles of O_3, NO_2, NO_3, and H_2O between 0 and 80km

On fig. 6.3-2 to 6.3-5, it is plotted the vertical profiles of O_3, NO_2, NO_3 and H_2O concentration for 2000 full dark measurements of cycle 22 (between 24/11/2003 and 29/12/2003, orbits between 9073 and 9573), between 0 and 80km.Tthe dataset is restricted to low latitudes (lower than 30°), for which variability should be lower, and to the most vertical occultations (parameter "verticality" lower than 30°). Furthermore, only non-flagged values are plotted. The number of profiles given on the figures is the number of profiles with at least one non-flagged value. We compare the global shape of all profiles by measurements from cold stars only (star temperature lower than 7000K), and of all profiles by measurements from hot stars only (star temperature higher than 7000K), in order to detect a possible impact of the star temperature on the vertical profiles.

For O_3 vertical profiles, globally on the whole range of altitude, there is no major difference between vertical profiles from hot stars and vertical profiles from cold stars. For NO_2 profiles, the dispersion of the values is higher for occultations from hot stars than for occultations from cold stars. For NO_3 profiles, the number of outliers is larger for hot stars than for cold stars at all altitudes. For H_2O profiles, there are no apparent outliers for vertical profiles from cold stars, whereas there are a very large number of outliers for vertical profiles from hot stars. Moreover, there are only a small number of non-flagged values at altitudes lower than 20km for occultations from hot stars.

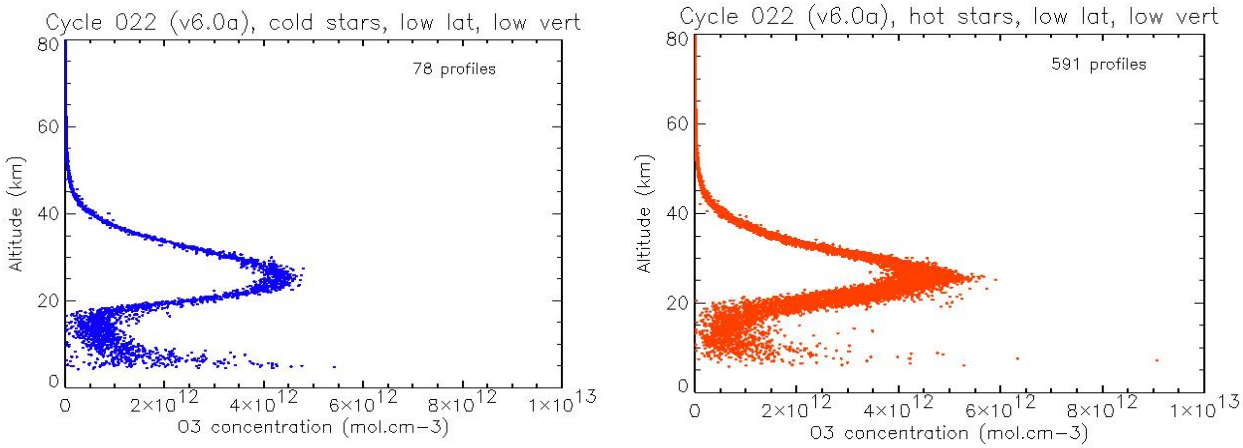

Figure 6.3-2: (Left) Concentration values of O_3 for 2000 full dark occultations of cycle 22 (GOPR v6.0a) between 0 and 80km altitude. Only measurements at low latitudes, nearly vertical and from occultations of cold stars (star temperature < 7000K) are considered. (Right) the same but for occultations of hot stars (star temperature > 7000K)

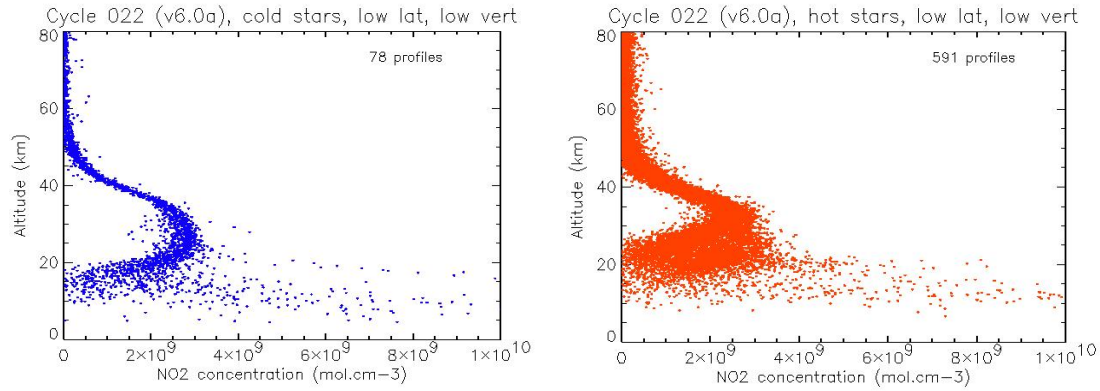

Figure 6.3-3: (Left) Concentration values of NO_2 for 2000 full dark occultations of cycle 22 (GOPR v6.0a) between 0 and 80km altitude. Only measurements at low latitudes, nearly vertical and from occultations of cold stars (star temperature < 7000K) are considered. (Right) the same but for occultations of hot stars (star temperature > 7000K)

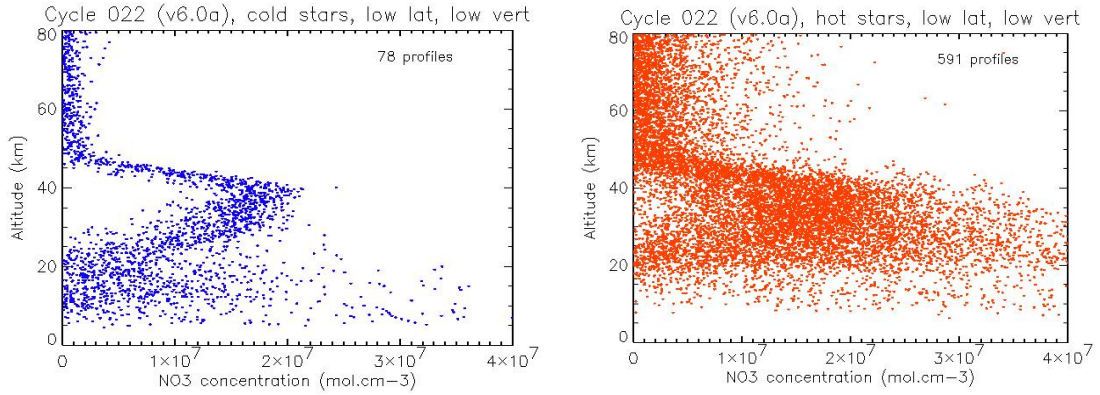

Figure 6.3-4: (Left) Concentration values of NO_3 for 2000 full dark occultations of cycle 22 (GOPR v6.0a) between 0 and 80km altitude. Only measurements at low latitudes, nearly vertical and from occultations of cold stars (star temperature < 7000K) are considered. (Right) the same but for occultations of hot stars (star temperature > 7000K)

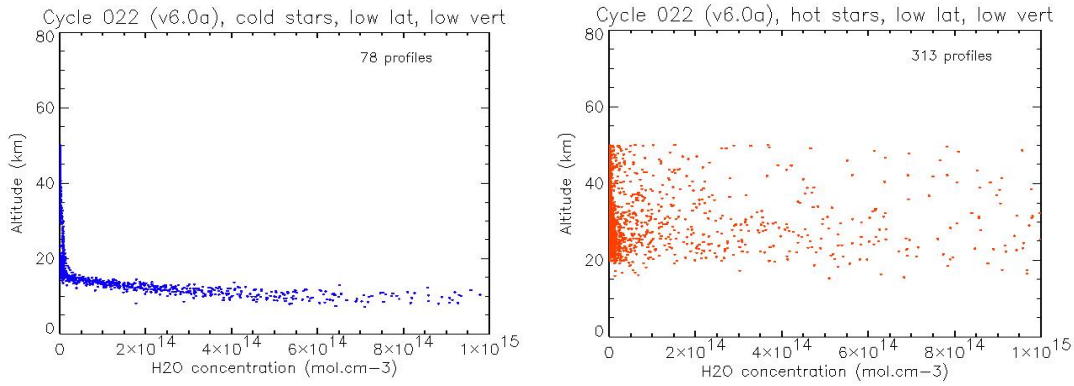

Figure 6.3-5: (Left) Concentration values of H_2O for 2000 full dark occultations of cycle 22 (GOPR v6.0a) between 0 and 80km altitude. Only measurements at low latitudes, nearly vertical and from occultations of cold stars (star temperature < 7000K) are considered. (Right) the same but for occultations of hot stars (star temperature > 7000K)

6.3.2.2 Vertical profiles of O_3 and H_2O in the upper stratosphere/mesosphere

At higher altitudes (Fig. 6.3-6 and 6.3-7), the comparison between cold and hot stars show that vertical profiles of O_3 include a few outliers between 40km and 80km for cold stars and almost none for hot stars. For H_2O vertical profiles between 40km and 50km, similarly to lower altitudes, the number of outliers for occultations of hot stars is much higher than for occultations of cold stars.

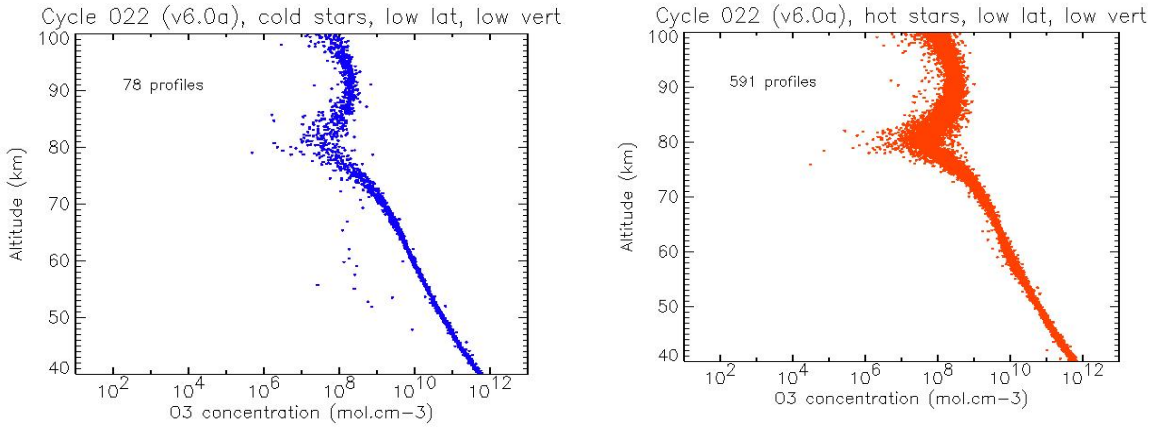

Figure 6.3-6: (Left) Concentration values of O_3 for 2000 full dark occultations of cycle 22 (GOPR v6.0a) between 40km and 100km altitude. Only measurements at low latitudes (lower than 30°), nearly vertical (parameter "verticality" lower than 30°) and from occultations of cold stars (star temperature lower than 7000K) are considered. Only non-flagged values are plotted. The number of profiles given is the number of profiles with at least one non-flagged value. (Right) The same but from occultations of hot stars (star temperature higher than 7000K)

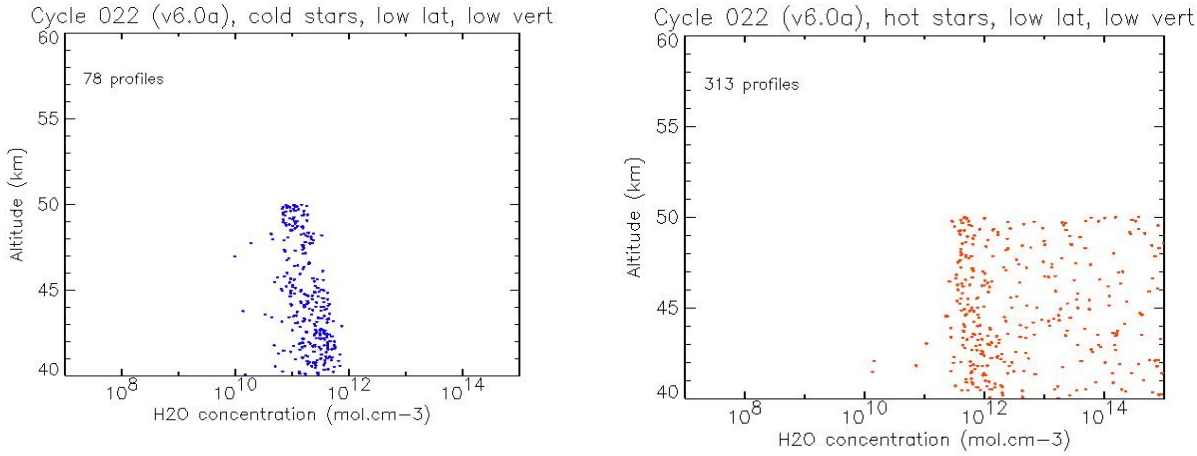

Figure 6.3-7: (Left) Concentration values of H_2O for 2000 full dark occultations of cycle 22 (GOPR v6.0a) between 40km and 100km altitude. Only measurements at low latitudes (lower than 30°), nearly vertical (parameter "verticality" lower than 30°) and from occultations of cold stars (star temperature lower than 7000K) are considered. Only non-flagged values are plotted. The number of profiles given is the number of profiles with at least one non-flagged value. (Right) The same but from occultations of hot stars (star temperature higher than 7000K)

6.3.3 INFLUENCE OF STAR MAGNITUDE ON VERTICAL PROFILES (GOPR V6.0A)

6.3.3.1 Vertical profiles of O_3, NO_2, NO_3, and H_2O between 0 and 80km

On fig. 6.3-8 to 6.3-11 it is plotted the vertical profiles of O_3, NO_2, NO_3 and H_2O for 2000 full dark measurements of cycle 22 (between 24/11/2003 and 29/12/2003, orbits between 9073 and 9573). We restrict the dataset to low latitudes (lower than 30°), for which natural variability is lower, and to the most vertical occultations (parameter "verticality" lower than 30°). Furthermore, only non-flagged values are plotted. The number of profiles given is the number of profiles with at least one non-flagged value. It is compared the global shape of all profiles by measurements from weak stars only (star magnitude higher than 1), and of all profiles by measurements from strong stars only (star magnitude lower than 1), in order to detect a possible impact of the star magnitude on the vertical profiles.

For O_3 vertical profiles, there is no major difference between the vertical profiles by strong stars and the vertical profiles by weak stars, except that there is a much smaller number of values (non-flagged values) at altitudes lower than 10 km for profiles measured from weak stars. For NO_2 profiles, it is obvious that the dispersion of the values at altitudes higher than 35km is lower for profiles from strong stars than from weak stars. The NO_3 profiles from strong stars are of better quality than those from weak stars. There is only a small number of non-flagged values at altitudes lower than 20km for profiles from weak stars. About H_2O profiles, only strong stars provide profiles with non-flagged values at altitudes lower than 20km. There is large number of outliers in both cases.

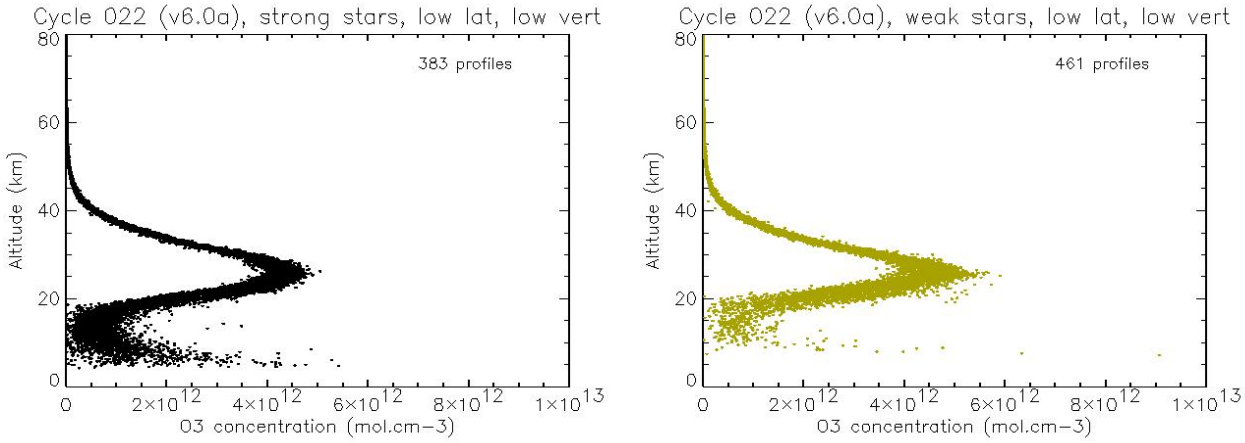

Figure 6.3-8: (Left) Concentration values of O_3 for 2000 full dark occultations of cycle 22 (GOPR v6.0a) vs altitude. Only measurements at low latitudes, nearly vertical and from occultations of strong stars (star magnitude < 1) are considered. (Right) The same but for measurements from occultations of weak stars (star magnitude > 1)

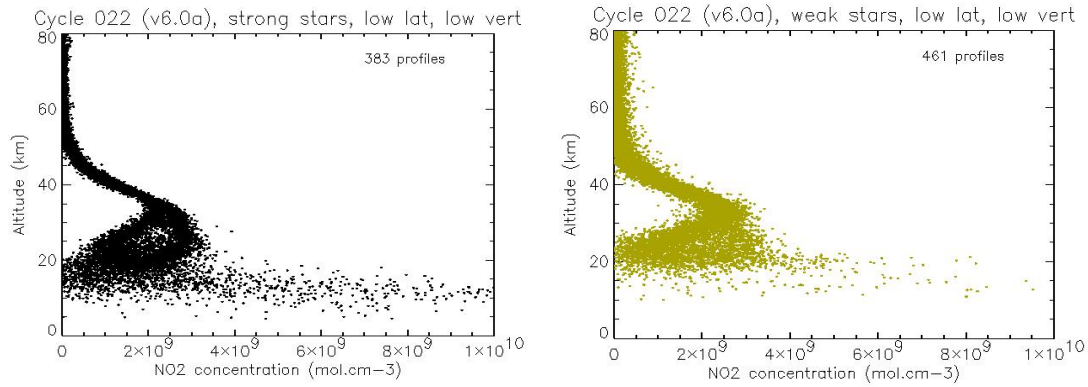

Figure 6.3-9: (Left) Concentration values of NO_2 for 2000 full dark occultations of cycle 22 (GOPR v6.0a) vs altitude. Only measurements at low latitudes, nearly vertical and from occultations of strong stars (star magnitude < 1) are considered. (Right) The same but for measurements from occultations of weak stars (star magnitude > 1)

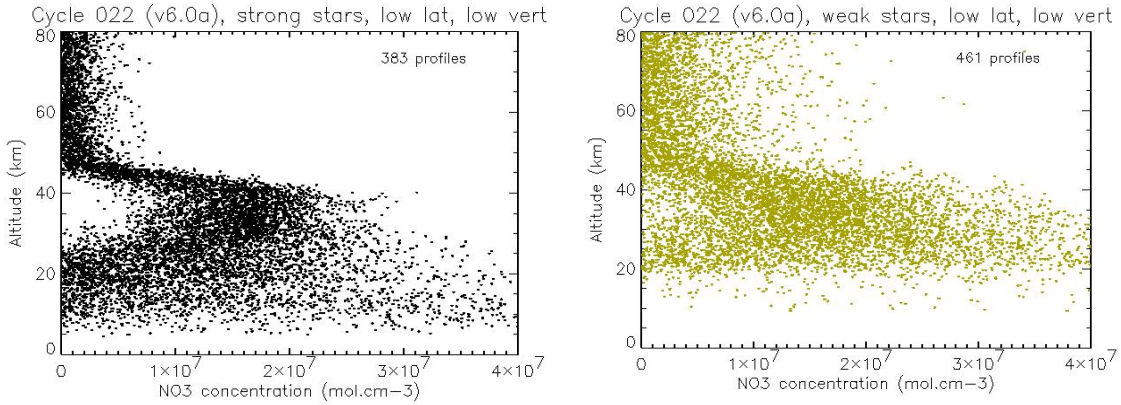

Figure 6.3-10: (Left) Concentration values of NO_3 for 2000 full dark occultations of cycle 22 (GOPR v6.0a) vs altitude. Only measurements at low latitudes, nearly vertical and from occultations of strong stars (star magnitude < 1) are considered. (Right) The same but for measurements from occultations of weak stars (star magnitude > 1)

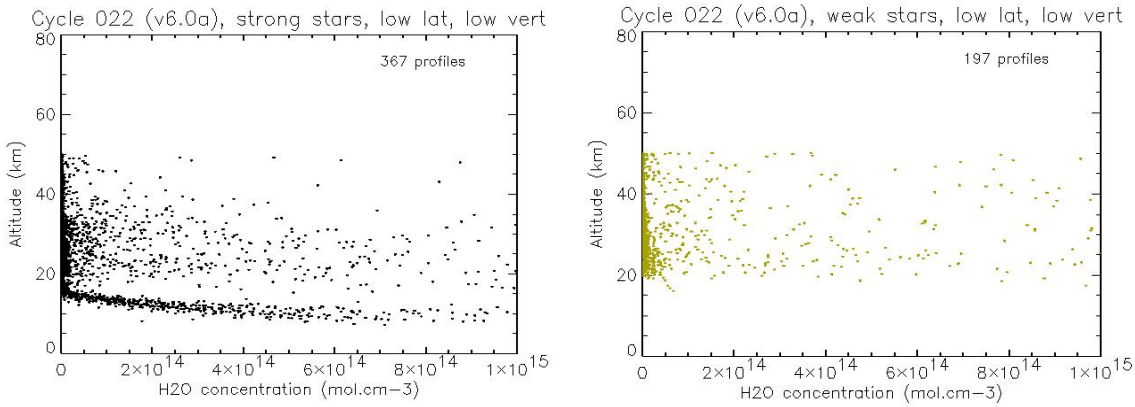

Figure 6.3-11: (Left) Concentration values of H_2O for 2000 full dark occultations of cycle 22 (GOPR v6.0a) vs altitude. Only measurements at low latitudes, nearly vertical and from occultations of strong stars (star magnitude < 1) are considered. (Right) The same but for measurements from occultations of weak stars (star magnitude > 1)

6.3.3.2 Vertical profiles of O_3 and H_2O in the upper stratosphere/mesosphere

At higher altitudes (fig. 6.3-12 and 6.3-13), there is no major difference between the behaviour of O_3 vertical profiles from occultations of strong stars and from occultations of weak stars. There is larger number of outliers for vertical profiles of H_2O from occultations of weak stars than from occultations of strong stars.

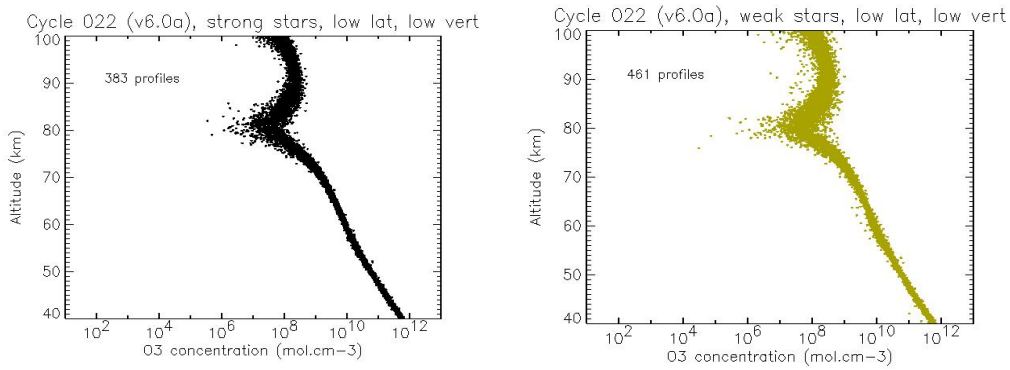

Figure 6.3-12: (Left) Concentration values of O_3 for 2000 full dark occultations of cycle 22 (GOPR v6.0a) between 40km and 100km altitude. Only measurements at low latitudes, nearly vertical and from occultations of strong stars are considered (star magnitude > 1). (Right) The same but for measurements from occultations of weak stars (star magnitude > 1)

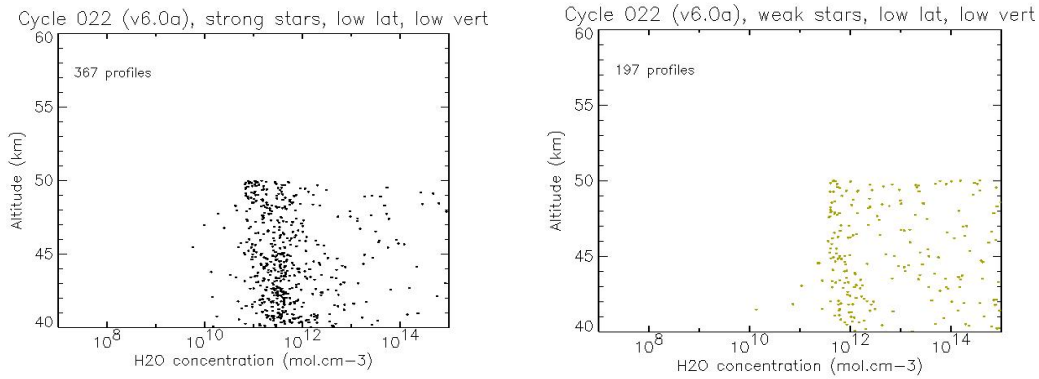

Figure 6.3-13: (Left) Concentration values of H_2O for 2000 full dark occultations of cycle 22 (GOPR v6.0a) between 40km and 100km altitude. Only measurements at low latitudes, nearly vertical and from occultations of strong stars are considered (star magnitude higher than 1). (Right) The same but for measurements from occultations of weak stars (star magnitude > 1)

6.3.4 O_3 QUALITY FOR FEW STARS

All dark limb Sirius occultations in 2003 are shown in fig. 6.3-14. This shows ozone results only. Column densities are shown in absolute units whereas local densities are shown in mixing ratios (ppm). The median values are shown by the red colour. These figures summarize 1111 measurements which differ widely by geographical location, date and verticality. The overall quality is good. The oblique occultations dominate Chi2 values below 40 km.

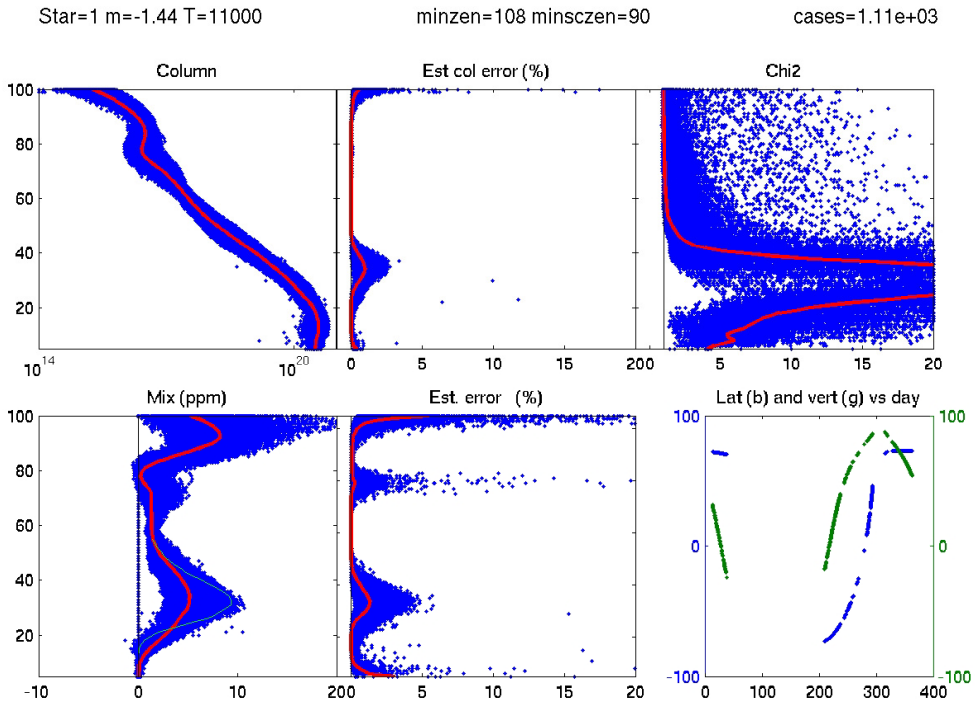

Figure 6.3-14: Dark limb Sirius occultations in 2003 are shown. Ozone results only

Fig. 6.3-15 plots the column and local densities for the Sirius occultations of fig. 6.3-14. The data points are divided into two groups according to the flagging status.

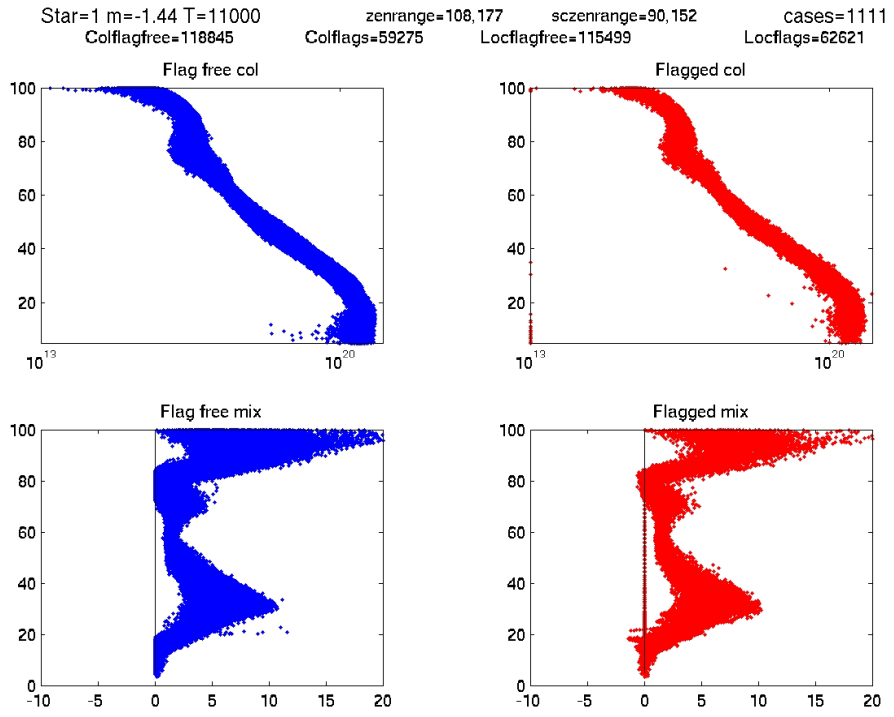

Figure 6.3-15: Ccolumn and local densities for the Sirius occultations of fig. 6.3-14

Fig. 6.3-16 and 6.3-17 are the same as fig. 6.3-14 and 6.3-15 respectively but for star 148 which is weak and cool. Ozone results look reasonable only up to 45 km (fig. 6.3-16).

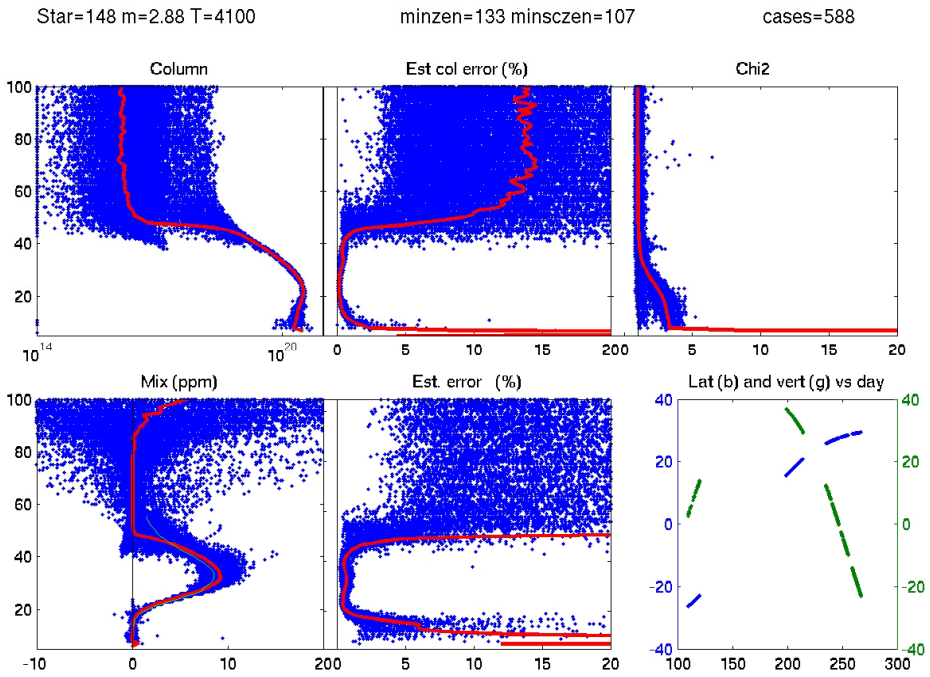

Figure 6.3-16: Same variables as fig. 6.3-14 but for star 148

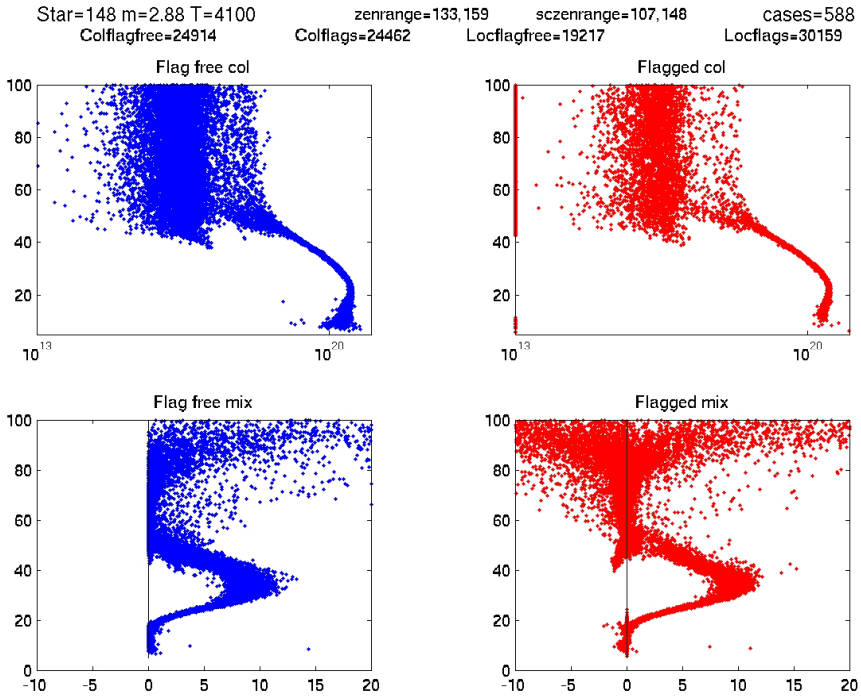

Figure 6.3-17: Flag picture for the star 148

7 VALIDATION ACTIVITIES AND RESULTS

7.1 GOMOS-ECMWF Comparisons: Temperature and Ozone

Due to restrictions in the current METEO product format, filtering of METEO data is not possible. ECMWF results are therefore partially based on data that are not to be used for scientific application, as mentioned in the disclaimer (http://envisat.esa.int/dataproducts/availability/disclaimers)

Summary of ECMWF GOMOS monthly report for December data (GOM_RR__2P):

- GOMOS temperature/ozone data gap between about 10S-30N and 30E-100E for most of the levels/layers and very few data between 0 and 5S.
- Overall good agreement between GOMOS and ECMWF temperatures.
- GOMOS temperatures are lower than ECMWF temperatures in most of the stratosphere and mesosphere, but area mean departures are less than 1% in most of the stratosphere. Larger departures are found in the mesosphere in particular at the model top.
- Large differences between GOMOS and ECMWF ozone values (over 50% in places).
- Large scatter of GOMOS ozone data.
- Scatter plots still show some unrealistically low GOMOS ozone values.
- No water vapor data in NRT GOMOS BUFR files.
- The monitoring statistics for December were produced with the operational ECMWF model, CY28R3.

The full December ECMWF report can be found in the links below:
http://earth.esa.int/pcs/envisat/gomos/reports/ecmwf_gomos_monthly_200412.pdf → text
http://earth.esa.int/pcs/envisat/gomos/reports/ecmwf_gomos_monthly_temp_200412.pdf → T plots
http://earth.esa.int/pcs/envisat/gomos/reports/ecmwf_gomos_monthly_o3_200412.pdf → O_3 plots

7.2 GOMOS-Climatology comparisons (n/a for this month)

Results will be presented upon availability.

7.3 GOMOS Assimilation (n/a for this month)

Results will be presented upon availability.

7.4 Consistency Verification: GOMOS-GOMOS Inter-comparison (n/a for this month)

Results will be presented upon availability.

7.5 Inter-Comparison with external data

7.5.1 COMPARISON OF O_3 VERTICAL PROFILES BY GOMOS AND BY SAGE III (GOPR V6.0A)

In this section it is compared GOMOS O_3 vertical profiles (GOPR v6.0a) with SAGE III O_3 vertical profiles (fig. 7.5-1). SAGE III data are courtesy of the NASA Langley Research Centre Atmospheric Sciences Data Centre. A GOMOS profile and a SAGE III profile are considered as coincident if measured within a distance of 100km and within a time difference of 12h.

Above the altitude of the maximum O_3 concentration, the difference between GOMOS and SAGE III profiles is higher than the error bars for some profiles (R07744/S027, R07749/S030, and R07769/S027). There is a major discrepancy about the amplitude of the O_3 maximum in three cases R07744/S027, R07749/S030 and R07771/S027. For other profiles, the difference between the maximum values by the 2 instruments is not significant when compared to the error bars and to the standard deviation. For R07910/S014, both instruments seem to capture the same small-scale features around 20-25km. At these altitudes, and at altitudes higher than the O_3 maximum, except for the cases mentioned above, we can not rule out a dynamical origin of the differences between GOMOS and SAGEIII. At lower altitudes, between 10km and 20km, the comparison is made more difficult due to the lower reliability of the instruments. There is some major discrepancy with SAGEIII measurements for three profiles (R07744/S027, R07770/S027 and R07910/S014. We can suspect a lower quality of GOMOS measurements at these altitudes for these specific profiles. But for other occultations (R07618/S023 and R07858/S014), the GOMOS O_3 profiles demonstrate the capacity of the instrument to provide good quality measurements down to at least 15km-10km.

For all GOMOS profiles presented on fig. 7.5-1, it is worth to note that no more random oscillations are present anymore in the O_3 concentration values, highlighting the strong improvement of the retrieval chain since the beginning of the CALVAL investigations.

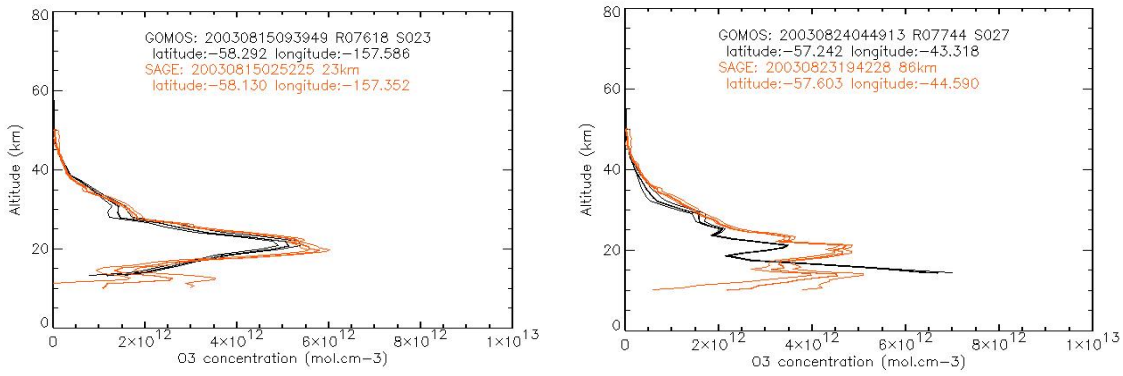

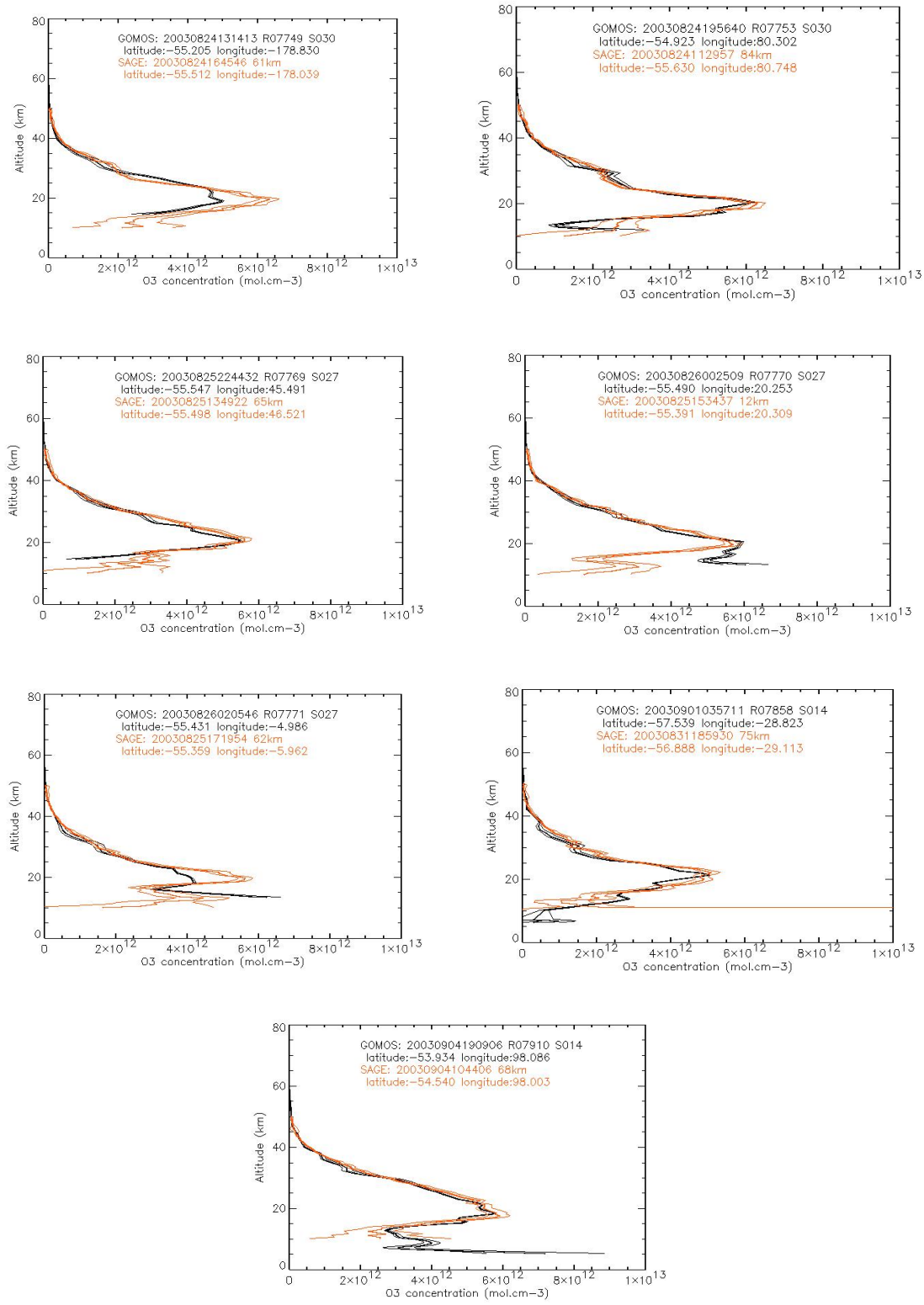

Figure 7.5-1: GOMOS vertical profiles of O_3 concentration (black thick line) and of its 1σ envelop (black thin lines) measured; coincident SAGEIII vertical profile of O_3 concentration (orange thick line) with error bars (orange thin lines). Date and location of the profiles, orbit and star for GOMOS and distance between the GOMOS and SAGEIII profiles are given on the figure.